USGS
science for a changing world

Prepared in cooperation with Bernalillo County Public Works Natural Resource Services

A Water-Budget Approach to Estimating Potential Groundwater Recharge From Two Domestic Sewage Disposal Fields in Eastern Bernalillo County, New Mexico, 2011–12

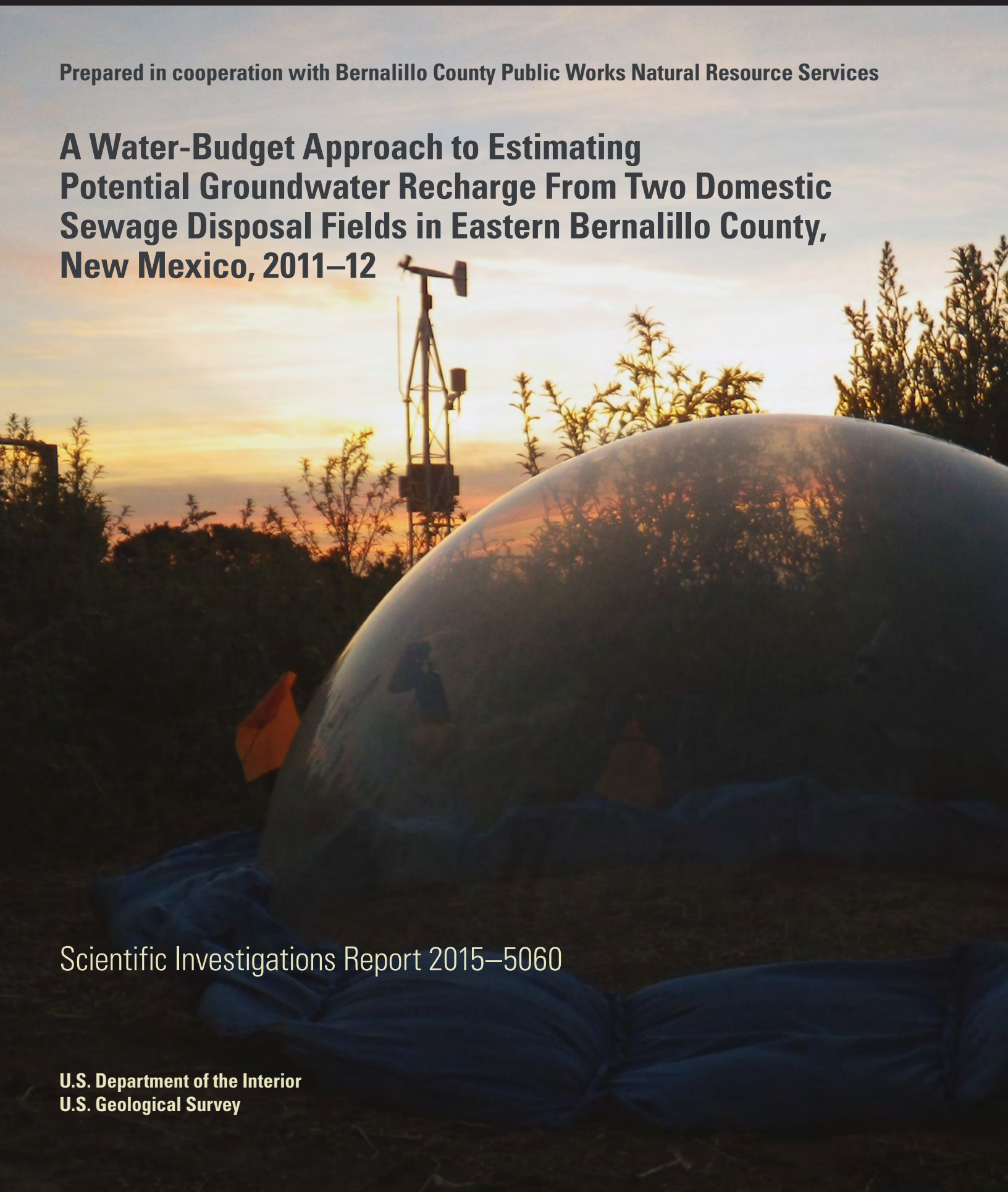

Scientific Investigations Report 2015–5060

U.S. Department of the Interior
U.S. Geological Survey

Cover.
A sunrise field visit to a disposal field located near the eastern edge of Bernalillo County, New Mexico, July 19, 2012, to conduct evapotranspiration measurements with a portable hemispherical evapotranspiration chamber.

A Water-Budget Approach to Estimating Potential Groundwater Recharge From Two Domestic Sewage Disposal Fields in Eastern Bernalillo County, New Mexico, 2011–12

By Dianna M. Crilley and Jake W. Collison

Prepared in cooperation with Bernalillo County Public Works
Natural Resource Services

Scientific Investigations Report 2015–5060

U.S. Department of the Interior
U.S. Geological Survey

U.S. Department of the Interior
SALLY JEWELL, Secretary

U.S. Geological Survey
Suzette M. Kimball, Acting Director

U.S. Geological Survey, Reston, Virginia: 2015

For more information on the USGS—the Federal source for science about the Earth, its natural and living resources, natural hazards, and the environment—visit http://www.usgs.gov or call 1–888–ASK–USGS.

For an overview of USGS information products, including maps, imagery, and publications, visit http://www.usgs.gov/pubprod/.

Suggested citation:
Crilley, D.M., and Collison, J.W., 2015, A water-budget approach to estimating potential groundwater recharge from two domestic sewage disposal fields in eastern Bernalillo County, New Mexico, 2011–12: U.S. Geological Survey Scientific Investigations Report 2015–5060, 32 p., http://dx.doi.org/10.3133/sir20155060.

ISSN 2328-0328 (online)

Acknowledgments

The authors gratefully acknowledge Bernalillo County Public Works Natural Resource Services for their cooperation with this investigation. The authors thank and acknowledge the valuable contributions from many individuals who assisted in this study, including Dan McGregor (Bernalillo County Public Works Natural Resource Services) for his support of this project and for his contributions of time, resources, and technical discussions; Chris Gonzales (Bernalillo County Public Works Natural Resource Services) for his assistance with selecting sites and improving our understanding of disposal field construction and design; and Eugene Bassett (E.C. Bassett Construction Company) for providing us with construction photographs, equipment specifications, and valuable ancillary data on the low-pressure dosing systems installed at the two sites included in this investigation. The authors also thank Jason Masoner and Kevin Smith (U.S. Geological Survey Oklahoma Water Science Center) for building and calibrating the evapotranspiration chamber, as well as for providing us with equipment and training; David Stannard (U.S. Geological Survey National Research Program) for his technical guidance on sample design and assistance with the complex equations used to compute evapotranspiration; and Scott Anderholm (retired hydrologist, U.S. Geological Survey New Mexico Water Science Center) for his guidance and conception of this project. Lastly, acknowledgment is due to the landowners of the two sites included in this investigation for graciously allowing us to conduct this study on their property.

Contents

Figures

Tables

Conversion Factors

International System of Units to Inch/Pound

Multiply	By	To obtain
	Length	
centimeter (cm)	0.3937	inch (in.)
millimeter (mm)	0.03937	inch (in.)
meter (m)	3.281	foot (ft)
kilometer (km)	0.6214	mile (mi)
	Area	
square meter (m^2)	10.76	square foot (ft^2)
	Volume	
liter (L)	0.2642	gallon (gal)
cubic meter (m^3)	264.2	gallon (gal)
cubic meter (m^3)	35.31	cubic foot (ft^3)
	Flow rate	
cubic meter per second (m^3/s)	35.31	cubic foot per second (ft^3/s)
cubic meter per day (m^3/d)	264.2	gallon per day (gal/d)
meter per hour (m/h)	39.37	inch per hour (in/h)
millimeter per year (mm/yr)	0.03937	inch per year (in/yr)
	Mass	
gram (g)	0.03527	ounce, avoirdupois (oz)
kilogram (kg)	2.205	pound avoirdupois (lb)
	Pressure	
kilopascal (kPa)	0.009869	atmosphere, standard (atm)
kilopascal (kPa)	0.01	bar
kilopascal (kPa)	0.2961	inch of mercury at 60 °F (in Hg)
	Density	
gram per cubic centimeter (g/cm^3)	62.4220	pound per cubic foot (lb/ft^3)
	Energy	
joule (J)	0.0000002	kilowatthour (kWh)
	Hydraulic conductivity	
meter per day (m/d)	3.281	foot per day (ft/d)

Temperature in degrees Celsius (°C) may be converted to degrees Fahrenheit (°F) as follows:

°F=(1.8×°C)+32

Temperature in degrees Fahrenheit (°F) may be converted to degrees Celsius (°C) as follows:

°C=(°F-32)/1.8

Vertical coordinate information is referenced to the North American Vertical Datum of 1929 (NAVD 29).

Horizontal coordinate information is referenced to the North American Datum of 1983 (NAD 83).

Elevation, as used in this report, refers to distance above the vertical datum.

Specific conductance is given in decisiemens per meter at 25 degrees Celsius (dS/m at 25 °C).

Concentrations of chemical constituents in water are given either in milligrams per liter (mg/L) or micrograms per liter (µg/L).

A Water-Budget Approach to Estimating Potential Groundwater Recharge From Two Domestic Sewage Disposal Fields in Eastern Bernalillo County, New Mexico, 2011–12

By Dianna M. Crilley and Jake W. Collison

Abstract

Eastern Bernalillo County, New Mexico, is a historically rural area that in recent years has experienced an increase in population and in the construction of new housing units, most of which are not connected to a centralized wastewater treatment system. Increasing water use has raised concerns about the effect of development on the available groundwater resources in the area. During 2011–12, the U.S. Geological Survey, in cooperation with Bernalillo County Public Works Natural Resource Services, used a water-budget approach to quantify the amount of potential groundwater recharge occurring from the domestic sewage (effluent) dosed to the sewage disposal field at two locations—sites A and B—in eastern Bernalillo County, N. Mex. The amount of effluent that is potentially available for groundwater recharge was determined as the mean daily volume of effluent dosed to the disposal field in excess of the mean daily volume of effluent loss from evapotranspiration from the disposal field.

During this study, the disposal fields at sites A and B received a measured volume of effluent from two-person domestic residences equipped with an onsite low-pressure dosing system. A combined evapotranspiration measurement and modeling technique was used to estimate the amount of evapotranspirative loss from the disposal field and from the surrounding terrain. A portable hemispherical flux chamber was used to measure evapotranspiration at fixed locations on the disposal fields and on the surrounding terrain at sites A and B. Data from hemispherical flux chamber measurements were used to calibrate a Penman-Monteith modeled evapotranspiration rate on the disposal field and on the surrounding terrain at site A from January 1, 2011, to December 31, 2011, and from January 1, 2012, to December 31, 2012, and at site B from January 1, 2011, to December 31, 2011. Micrometeorological and soil data from instrumentation on the disposal fields and on the surrounding terrain at sites A and B were used as input data into the Penman-Monteith equation. The mean potential recharge from disposal field effluent during 2011–12 at sites A and B was 63 percent of the volume of effluent dosed to the disposal field.

Introduction

Natural groundwater recharge (recharge) primarily occurs from the infiltration of precipitation; however, in arid and semiarid regions, evaporation can exceed precipitation, resulting in little or no recharge. In semiarid regions of the southwestern United States, the drainage of wastewater (effluent) from sewage disposal fields (disposal fields) can be an important contribution to recharge. Few studies have quantified the amount of effluent drainage from individual disposal fields. Estimates of potential recharge from disposal fields can be critical for water-resource planning and management in water-stressed regions.

During 2011–12, the U.S. Geological Survey (USGS), in cooperation with Bernalillo County Public Works Natural Resource Services, used a water-budget approach to quantify the potential recharge from two domestic disposal fields (sites A and B; fig. 1) located in eastern Bernalillo County, New Mexico. The study area is located on the eastern side of the Sandia and Manzanita Mountains, an area commonly referred to as the "East Mountain area" (EMA). The EMA is a historically rural area; the 1990 U.S. Census reported that 99 percent of households in the EMA were not connected to a centralized wastewater treatment system and therefore relied on individual sewage disposal systems for the treatment and removal of domestic effluent (U.S. Census Bureau, 1990). In recent years, the EMA has become part of the rapidly growing greater Albuquerque metropolitan area. Between 1970 and 2010, the population of eastern Bernalillo County increased from about 4,000 to more than 19,000, and housing units increased from about 1,500 to more than 9,000 (Blanchard and Kues, 1999; U.S. Census Bureau, 2010). Increased domestic water use has raised concerns about the effect of development on the available groundwater resources in the area.

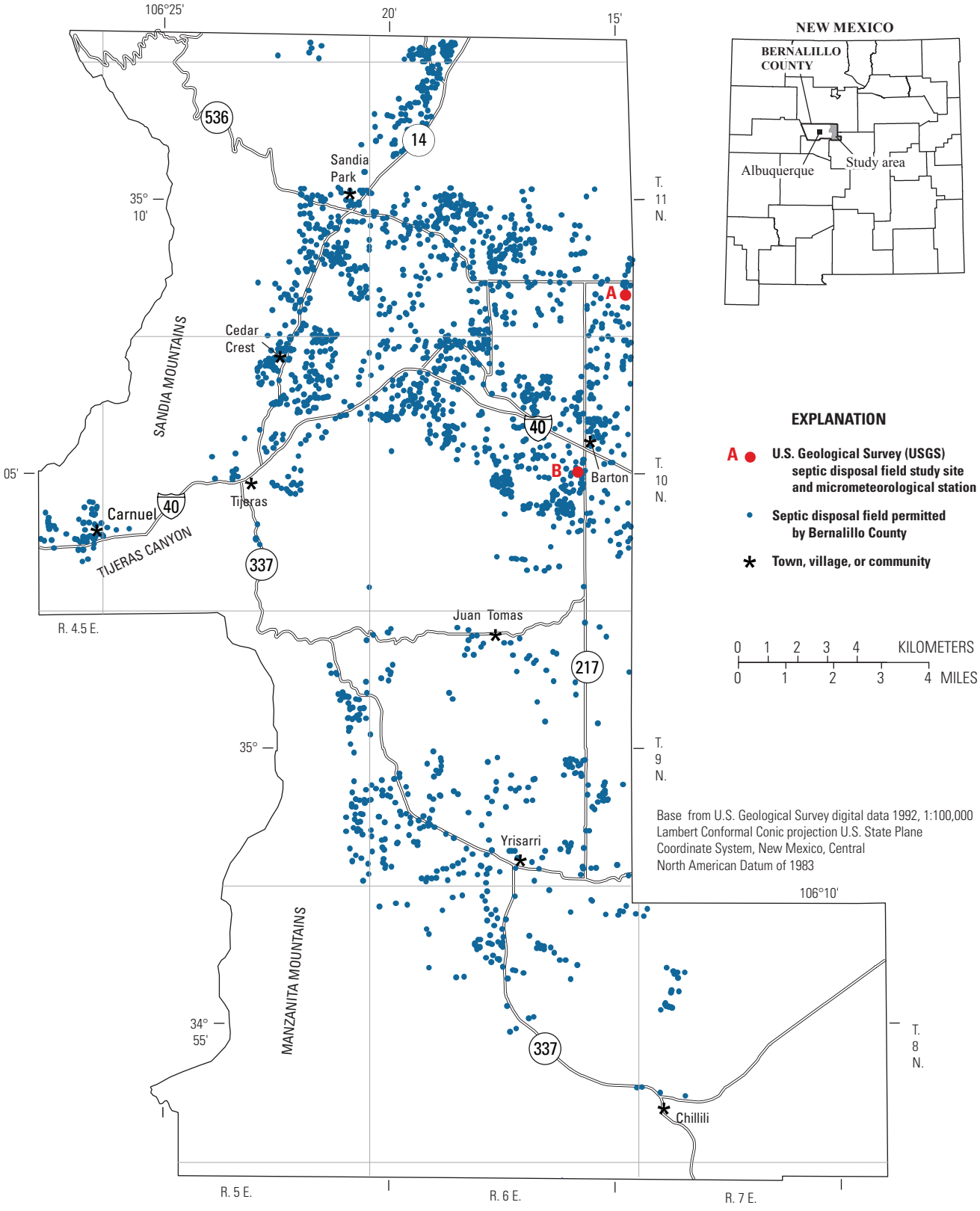

Figure 1. The study area showing the location of data-collection sites and the spatial distribution of permittted sewage disposal fields in eastern Bernalillo County, New Mexico, 2012.

Recharge in the EMA results from the infiltration of local or regional precipitation, snowmelt in the high elevation areas of the Sandia and Manzanita Mountains, groundwater inflow from adjacent groundwater basins, and drainage of effluent from sewage disposal fields (Bartolino and others, 2010). As of 2013, there were approximately 1,600 permitted disposal fields (fig. 1) (Bernalillo County Public Works Natural Resource Services, 2013) and an estimated 2,000 unpermitted disposal fields in eastern Bernalillo County (Dan McGregor, Bernalillo County Public Works Natural Resource Services, written commun., 2013), for a total of about 3,600 disposal fields. The number of unpermitted disposal fields in eastern Bernalillo County was estimated by Bernalillo County Public Works Natural Resource Services in a campaign implemented to assess the number of unpermitted sewage disposal systems through a comparison of geographic information system data and the Bernalillo County Liquid Waste Permit Database.

A disposal field is designed to dispose of effluent through drainage and evapotranspiration (ET, evaporation from the land surface and transpiration by plants). A disposal field water budget reflects the balance between the inputs (gains) and outputs (losses) of hydrologic components to and from the disposal field (fig. 2). Hydrologic gains to the disposal field include the infiltration of precipitation and effluent drainage. When gains to the disposal field exceed ET losses, there is a potential for recharge from the disposal field. Potential recharge in this report is defined as the excess of precipitation and effluent over evapotranspiration. Potential recharge from the infiltration of precipitation and the drainage of effluent through the subsurface may become recharge, or it may be later consumed by evapotranspiration and (or) remain in the unsaturated zone as storage (Healy, 2010).

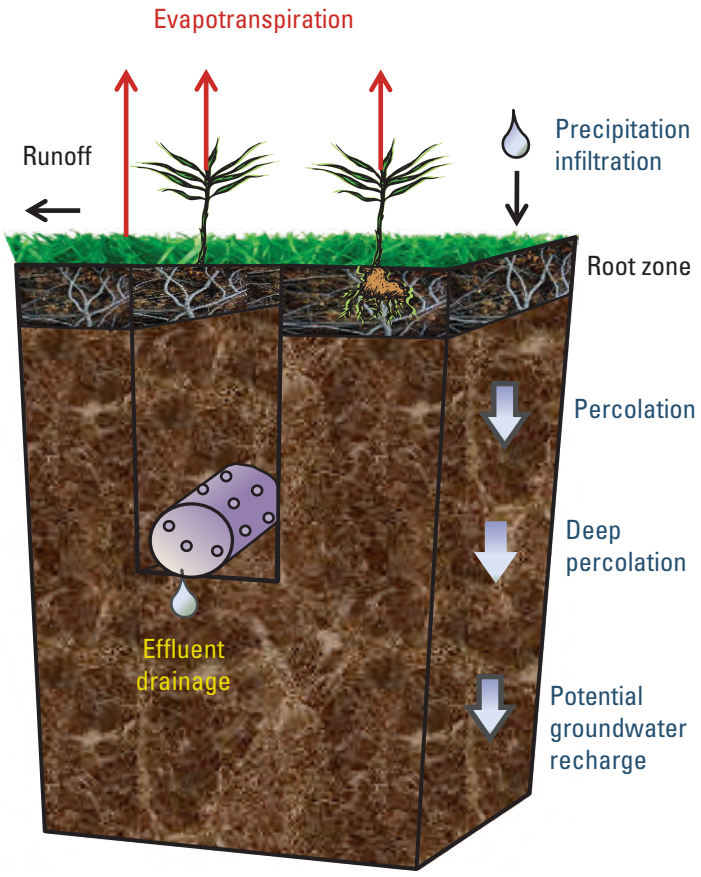

Figure 2. The hydrologic components of a disposal field, including precipitation infiltration, effluent drainage, evapotranspiration, runoff, percolation, and potential groundwater recharge.

Purpose and Scope

The purpose of this report is to describe the use of a water-budget approach to estimate the amount of potential recharge from two domestic disposal fields in the EMA. The scope of this report describes the sampling and assessment methodology used to evaluate the water-budget components of the two domestic disposal fields and their surrounding terrain for the period 2011–12. Information from this study can be used by water-resource managers to obtain a better understanding of the quantity of potential recharge resulting from the drainage of effluent from disposal fields, as well as the importance of recharge from disposal fields to the hydrologic budget in semiarid climates.

Description of Study Area

The study area is about 675 square kilometers in eastern Bernalillo County, N. Mex., including part of the EMA and encompassing the eastern side of the Sandia and Manzanita Mountains (fig. 1). Sites A and B are located in the eastern, lower elevation parts of the EMA, which have a semiarid climate according to a modified Thornthwaite climate classification by Tuan and others (1969). In semiarid climates, annual ET can exceed annual precipitation; for example, a mean total pan evaporation of 1,412 millimeters per year (mm/y) (Western Regional Climate Center, 2013a) and a mean annual precipitation of 325 mm/y (Western Regional Climate Center, 2013b) from 1914 to 2005 were recorded at the National Oceanic and Atmospheric Administration (NOAA) Cooperative Observer Network station 293060 in Estancia, N. Mex. (1,840 meters [m] above National Geodetic Vertical Datum of 1929 [NGVD29]; not shown on fig. 1), located approximately 40 kilometers (km) southeast of Barton, N. Mex. Precipitation events in the EMA can be highly localized, resulting in a large degree of spatial and interannual variability in precipitation. The wettest months of the year are July and August, with eastern, lower elevation areas of the EMA receiving approximately 30 percent of the annual precipitation during these months from localized monsoonal storms. The majority (54 percent) of annual precipitation in the EMA occurs from regional frontal storms during the winter

months. The driest months of the year are typically April, May, and June, during which approximately 16 percent of the total precipitation occurs (Bartolino and others, 2010). During 2011 and 2012, local climate data were recorded by the USGS at disposal field sites A and B (fig. 1). (Data at sites A and B are archived and are available by request from the USGS New Mexico Water Science Center, Albuquerque, N. Mex.) In general, 2012 was drier than 2011, with about 260 millimeters (mm) of precipitation occurring during 2011 and about 160 mm of precipitation occurring during 2012. The annual mean air temperature in 2012 was about 1 degree Celsius (°C) warmer than in 2011, with the monthly mean air temperature during 2011 and 2012 ranging from a low of 2.4 °C in December 2011 to a high of 22.5 °C in July 2011. During the study, the prevailing wind direction ranged from northwest to northeast, and the monthly mean wind speed ranged from a low of 1.9 meters per second (m/s) in July 2011 to a high of 3.8 m/s in April 2011.

Previous Studies

A review of previous investigations indicated that few studies have quantified potential recharge from disposal fields in semiarid regions. Additionally, few data exist that can be used to quantify ET loss from disposal fields in semiarid regions. In New Mexico, water budgets developed by resource managers generally assume that about half of the total amount of domestic water supplied to a residence with a sewage disposal system is lost as evaporation or transpiration; the remaining half would be available to recharge area aquifers (Wilson and Lucero, 1997; McQuillan and Bassett, 2009). The New Mexico Office of the State Engineer (NMOSE), which assesses water use in New Mexico, defines groundwater depletion as

> That part of a [groundwater] withdrawal that has been evaporated, transpired, incorporated into crops or products, consumed by man or livestock, or otherwise removed from the water environment. It includes that portion of ground water [sic] recharge resulting from seepage or deep percolation (in connection with a water use) that is not economically recoverable in a reasonable number of years, or is not usable (Wilson and others, 2003).

In a report from NMOSE on water use by categories in New Mexico by Wilson and others (2003), the amount of aquifer depletion from domestic water use by residences with a sewage disposal system was estimated by multiplying groundwater withdrawals by a depletion factor of 1.0. The NMOSE defines the depletion factor as the percentage of the water being depleted that is unavailable for additional use, with a depletion factor of 1 being 100 percent depletion and a depletion factor of 0 being no depletion. Wilson and others (2003) stated that in previous "NMOSE New Mexico Water Use by Categories" reports, a depletion factor of 0.45 had been used, but recently a more conservative factor of 1.0 had been adopted because of increasing evidence that recharge from disposal fields rarely reach the aquifers. The evidence for this decision by the NMOSE was not cited; however, Wilson and others (2003) did note that assuming a depletion factor of 1.0 can involve a high degree of uncertainty depending on site conditions such as depth to groundwater, depth to bedrock, installation depth of disposal field, and soil type.

In a hearing before the NMOSE Hearing Office regarding a request for return flow (recharge from effluent) credit within the Roswell, N. Mex., underground water basin, the NMOSE concluded through findings by Atkins Engineering Associates that 85 percent of the effluent discharged to a disposal field percolated through the unsaturated zone to the shallow aquifer (34 m deep) (New Mexico Office of the State Engineer, 2001). Blandford (2006) used the hydraulic properties of soil borings collected from disposal fields in Roswell, N. Mex., in conjunction with numerical simulations, to quantify recharge from the disposal fields. The results of the Blandford (2006) study indicated that 47 percent of the domestic water supplied to a residence was available for recharge. Bartolino and others (2010) estimated that, for the entire EMA (about 1,040 square kilometers), the amount of potential recharge resulting from the drainage of effluent from disposal fields was about 1,475 acre-feet per year, on the basis of the assumption that 45 percent of water supplied to a residence resulted in recharge determined by Wilson and Lucero (1997).

In a study conducted in Lubbock, Texas, by Rainwater and others (2005), nine artificial disposal fields were constructed to quantify ET and drainage losses from the disposal fields by using three different types of controls: (1) 3 disposal fields permitted ET losses only (ET fields), (2) 3 disposal fields permitted drainage losses only (drainage fields), and (3) 3 disposal fields permitted ET and drainage losses (ET and drainage fields). The amount of effluent required to maintain saturation of the disposal fields within 20 centimeters (cm) of the land surface averaged 25 liters per day (L/d) at the ET fields, 260 L/d at the drainage fields, and 430 L/d at the ET and drainage fields. The drainage fields required about 10 times more effluent than the ET fields to maintain saturation, indicating that effluent loss (under controlled saturation levels) from disposal field drainage is substantially greater than effluent loss from ET.

A disposal field study by Stannard and others (2010) in western Jefferson County, Colorado, found that approximately 91 percent of effluent that entered the disposal field annually was potentially available for recharge. Stannard and others (2010) determined potential recharge by using a water-budget approach in conjunction with a combined ET measurement and modeling technique on the disposal field and on the adjacent natural terrain (surrounding terrain). The study described in this report employed a similar approach to determine potential recharge from two disposal fields by using suggestions and recommendations from Stannard and others (2010).

Study Design and Methods

A simple water budget was used to estimate the mean daily volume of water potentially available for recharge. This approach (see "Water-Budget Approach" section) is an input-output accounting technique where known or measurable water-budget components can be used to solve for an unknown or unmeasured component. In this study, three water-budget components were considered: (1) the volume of effluent dosed to a disposal field, (2) the volume of effluent lost through ET from the disposal field, and (3) the volume of effluent potentially available for recharge. The volume of effluent dosed to the disposal field was calculated by using the dimensions of the septic tank and the change in effluent level inside the tank (see "Data Collection and Methods of Effluent Dose Estimation" section). The amount of effluent loss through ET from the disposal field was estimated as the amount of ET loss from the disposal field in excess of ET loss from the surrounding terrain. Evapotranspiration was estimated by using a combined measurement and modeling technique (see "Data Collection and Methods of Evapotranspiration Estimation" section) modified from Stannard and others (2010).

Site Selection and Characterization

The two study locations selected for this investigation were site A, located north of Interstate 40 near the eastern edge of Bernalillo County, N. Mex., and site B, located south of Interstate 40 near Barton, N. Mex. (fig. 1). Sites A and B are disposal fields located approximately 6 km apart and at about the same elevation, approximately 2,103 meters (m) and 2,109 m above NGVD 29, respectively (table 1). In this study, two sites with similar site characteristics were investigated to provide added confidence in study results. The similarities in site conditions at sites A and B included the size of the residence, the type of soil, the young age (approximately 5 years old) of the disposal fields, and the use of a pumped sewage disposal system. Sites were also selected on the basis of the ease of accessibility and the suitability of siting a weather station.

The residents at sites A and B obtain their water from a local public water supplier, the Entranosa Water and Wastewater Association, Tijeras, N. Mex. Although these residences are serviced by a public water supplier, they are not serviced by a centralized sewage disposal system and therefore rely on onsite sewage disposal systems to remove domestic wastewater. The residence at site B also utilized a home water softener treatment system.

During this study, the disposal fields at sites A and B received effluent from a two-person domestic residence equipped with an onsite low-pressure dosing system (LPDS), which is a type of pumped sewage disposal system, installed in 2006 at site A and in 2007 at site B (fig. 3). The LPDS at sites A and B are low head pressure (about 0.8–1.5 m of pressure head) effluent-collection and treatment systems that include several narrow (approximately 30 cm) and shallow (0.9–1.5 m) trenches, with each trench containing an effluent-distribution line installed at approximately 45-cm depth that receives periodic and uniformly distributed doses of effluent. The LPDSs are designed to promote ET and aerobic conditions while minimizing loss of soil permeability caused by site disturbance (U.S. Environmental Protection Agency, 1999). The LPDSs installed at sites A and B also included a pump control telemetry system (VeriComm Monitoring System, Orenco Wastewater Solutions, Sutherlin, Oregon) to conduct Web-based monitoring of the operation of the pump deployed in the septic tank. Although LPDSs only account for about 37 percent of disposal fields in eastern Bernalillo County, this study selected disposal fields with LPDSs specifically because they allowed for easy and more accurate measurement of the volume of effluent dosed when compared to gravity-fed sewage disposal systems, which account for the remaining 63 percent of disposal fields in eastern Bernalillo County (Bernalillo County Public Works Natural Resource Services, 2013).

At sites A and B, effluent was discharged from each residence to a primary settling tank—1 of 2 inline 5,678-liter double-compartment concrete septic tanks installed at each site—obtained from Albuquerque Vault Company, Albuquerque, N. Mex. The overflow of effluent from the primary septic tank was directed to the secondary septic tank.

Table 1. Selected information on sites included in this study, eastern Bernalillo County, New Mexico.

[NAD 83, North American Datum of 1983; m, meters; NGVD 29, National Geodetic Vertical Datum of 1929; m^2, square meter; °, degrees; ', minutes; LPDS, low pressure dosing system]

Station	Period of data collection	Latitude (NAD 83)	Longitude (NAD 83)	Elevation (m above NGVD 29)	Sewage disposal system		Disposal field (m)		Effluent drainage area (m^2)
					Type	Installation date	Length	Width	
Site A	2011, 2012	35°08'	106°16'	2,103	LPDS	2006	18.3	6.4	117.1
Site B	2011	35°05'	106°15'	2,109	LPDS	2007	18.3	4.9	89.7

Figure 3. The location of the house, septic tanks, disposal field, and data-collection instrumentation at *A*, site A, and *B*, site B.

When the effluent level in the secondary septic tank reached an upper trigger point, a submersible pump was activated, and effluent was pumped from the secondary septic tank to the disposal field (fig. 4). The pumping of effluent ceased when the effluent level in the second tank reached a lower trigger point, deactivating the submersible pump and ending the pump cycle.

On the disposal field, a distribution box alternated the flow of effluent from the septic tank to one of several effluent-distribution lines buried in lateral trenches (fig. 5). On average, each effluent-distribution line received effluent once a day; the daily volume of effluent distributed to the lateral trenches is discussed in the section "Data Collection and Methods of Effluent Dose Estimation." The effluent-distribution lines were constructed of 5.08-cm- (2-inch [in.]) diameter polyvinyl chloride (PVC) tubing with 6.35-mm- (0.25-in.) diameter orifices, housed inside perforated 10.16-cm- (4-in.) diameter PVC tubing, and packed in a 30.5-cm- (12-in.) diameter expanded polystyrene bundle (EZflow, Infiltrator Systems Inc., Old Saybrook, Connecticut; fig. 5*C*). Lateral trenches can contain one or more expanded polystyrene bundles stacked below the effluent-distribution line to increase drainage depth. In each lateral trench, the uppermost expanded polystyrene bundle, which contained the effluent-distribution line, was buried approximately 30 cm below land surface and backfilled with native soil, such that the effluent-distribution line was approximately 45 cm below land surface.

The site A disposal field contained three 18.3-m-long effluent-distribution lines spaced 3.20 m apart for an effluent drainage area of 117.1 square meters (m^2) (fig. 5*A*; table 1). The total depth of the lateral trenches at site A was 1.5 m below land surface, with each trench containing four stacked expanded polystyrene bundles and backfilled to the land surface with native soil. The site B disposal field contained four 18.3-m-long effluent-distribution lines spaced 1.63 m apart for an effluent drainage area of 89.7 m^2 (fig. 5*B*; table 1).

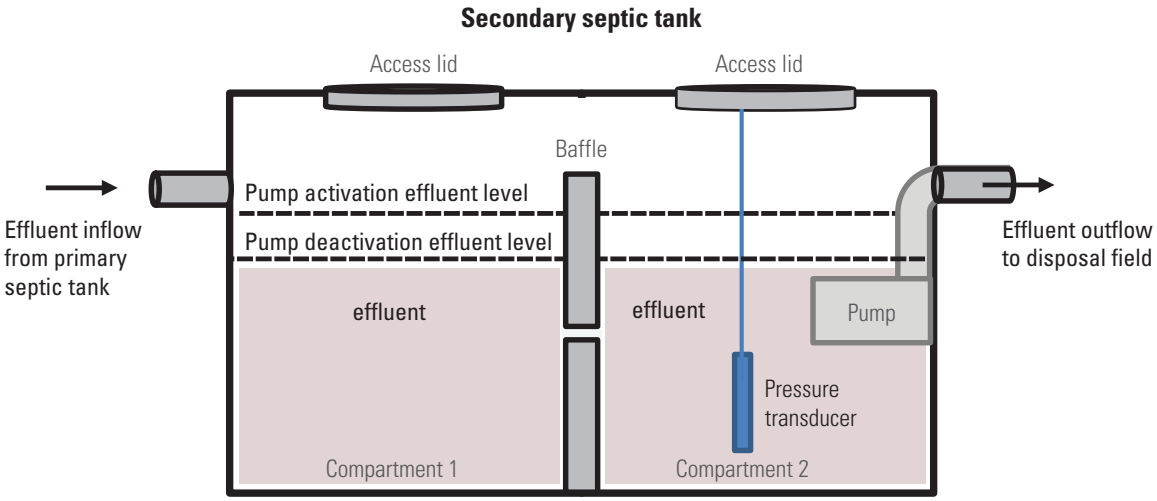

Figure 4. The design of the secondary, double-compartment septic tank; the effluent-level trigger points that control pump activation and deactivation; and the location of the pressure transducer.

The total depth of the lateral trenches at site B was 0.9 m below land surface, with each trench containing two stacked and expanded polystyrene bundles and backfilled to the land surface with native soil.

The general location of the effluent-distribution lines on the disposal fields at sites A and B were easily identified from surficial access ports to the distribution-box cover and to the flush-out ports at the distal end of each effluent-distribution line and from the relative abundance of vegetative cover when compared to the surrounding terrain (fig. 6*A–D*). The vegetative cover at site A on September 12, 2011; November 30, 2011; May 19, 2012; and July 14, 2012 is shown in figures 6*A–D*, respectively. Photographs were taken at site A near the south end of the disposal field looking north, with the white flush-out ports of the disposal field shown in the foreground of the photographs. During the growing season (defined here as March 15 to November 15), vegetation on the disposal fields at sites A and B typically covered 50–90 percent of the ground on the basis of leaf area index estimates (a discussion of this methodology is given in the section "Leaf Area Index Data Collection and Estimation"), with dominant vegetation including various *Aristida* sp. (three-awn grasses), *Pascopyrum smithii* (western wheatgrass), and *Salsola tragus* L. (prickly Russian thistle). The distribution of vegetation along the length and width of the disposal fields was fairly homogeneous throughout the year; however, the density and height of vegetation on the disposal field varied with seasons. Vegetative cover during the months of May, July, August, and September was generally denser and taller than vegetative cover during other months of the year. On the surrounding terrain, the percentage of vegetative cover during the growing season at sites A and B was typically 20 percent, with dominant vegetation including various *Bouteloua* sp. (grama grasses), *Muhlenbergia torreyi* (ring muhly), family *Cactaceae* (cacti), *Juniperus monosperma* (one seed Juniper), and *Pinus ponderosa* (ponderosa pine). The surrounding terrain at site A had a one seed juniper tree (approximately 2 m tall) near the east edge of the disposal field, and the surrounding terrain at site B had a ponderosa pine-dominated copse of trees (approximately 4 m tall) near the southwest corner of the disposal field. The copse of trees on the surrounding terrain at site B is noteworthy because it shades the western side of the disposal field.

Annually, the occurrence of vegetative growth on the disposal fields and the surrounding terrain followed a bimodal response curve where growth peaked twice during the year—once during the spring, following winter snowmelt, and once during late summer, following monsoonal storms (see "Leaf Area Index Data Collection and Estimation" section). During this study, the natural vegetative cover on the disposal fields and on the surrounding terrain at sites A and B was undisturbed, such that no intentional lawn maintenance was performed. The only exception to this was in June 2011, when drought conditions and an increased risk of wildfire from the dry brush required mowing of the disposal field at site A.

The general soil taxonomy of the area encompassing sites A and B is classified by the U.S. Department of Agriculture (2012) as an aridisol and includes the Silver (55–60 percent) and Witt (25–30 percent) soil series compositions. The amount of water potentially stored in Silver and Witt soil that may be available for uptake by plants to a rooting depth of 1.5 m or more ranges from 18 to 21 percent and was calculated as the difference between the upper (field capacity) and the lower (permanent wilting point) limits of water storage (U.S. Department of Agriculture, 2012). The color and texture of the Silver and Witt soil series can be brown to yellowish brown, very fine, sandy loam from zero to 12.7 cm below land surface and brown to reddish brown, silty clay loam from 12.7 to 76.2 cm below land surface (U.S. Department of Agriculture, 2012).

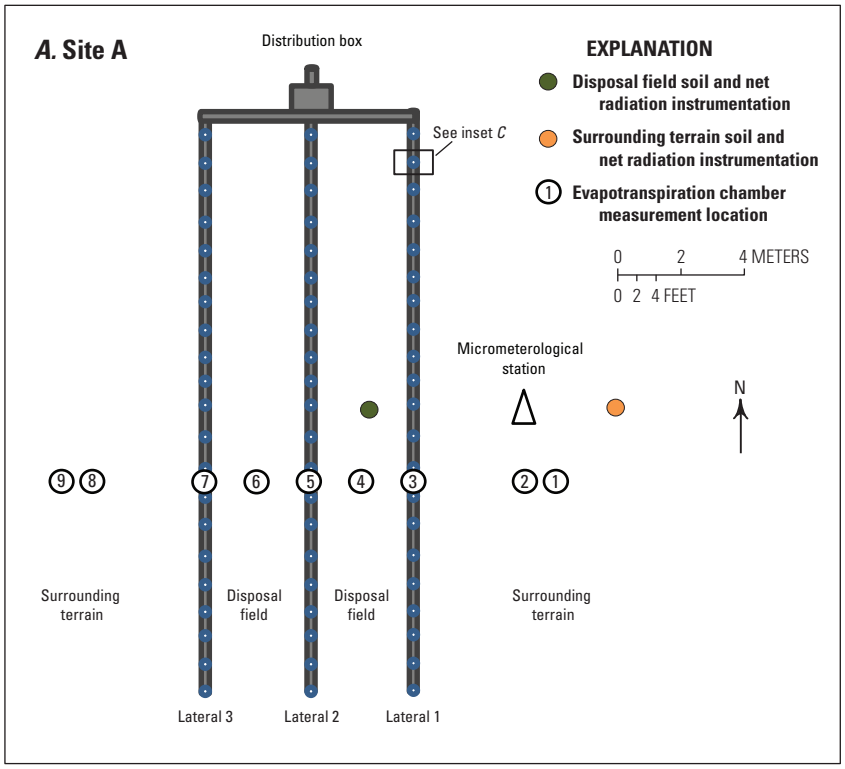

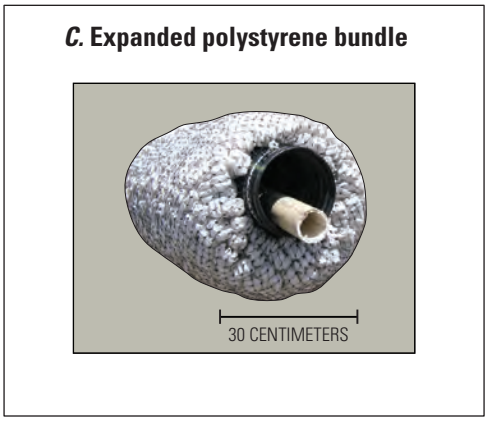

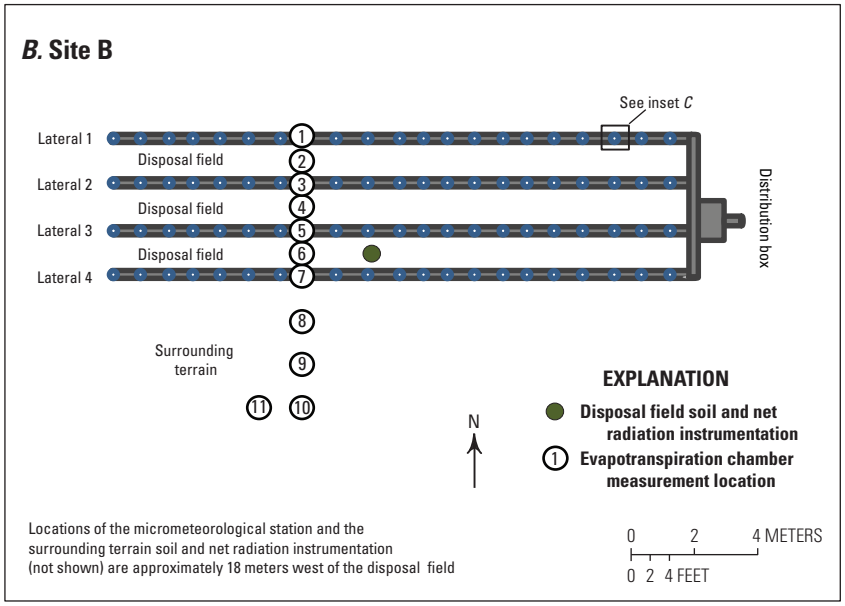

Figure 5. The locations of the evapotranspiration chamber measurements relative to the disposal field effluent-distribution (lateral) lines and data-collection instrumentation at *A*, site A; *B*, site B; and inset *C*, showing an expanded polystyrene bundle.

A. **September 12, 2011**

B. **November 30, 2011**

C. **May 19, 2012**

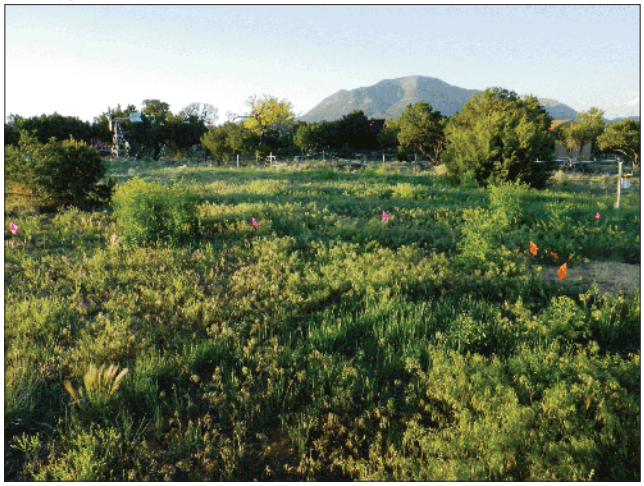

D. **July 14, 2012**

Figure 6. Vegetation at site A on *A*, September 12, 2011; *B*, November 30, 2011; *C*, May 19, 2012; and *D*, July, 14, 2012.

Sieve and hydrometer methods (Das, 2009) were used to determine the grain-size distribution of composited soil samples collected at sites A and B from the disposal fields and surrounding terrain. Soil samples were collected from zero to 15.2 cm below the land surface at locations on the disposal field and surrounding terrain and from 15.2 to 30.5 cm and 30.5 to 45.7 cm below the land surface at locations on the surrounding terrain. Results from the grain-size distribution analysis are presented in table 2. At sites A and B, the soil texture of the disposal fields was classified as loam, whereas soil texture of the surrounding terrain at zero to 15.2 cm below the land surface was classified as sandy clay loam, on the basis of the U.S. Department of Agriculture Textural Soil Classification Study Guide (U.S. Department of Agriculture, 1987). Soil samples from the disposal fields and surrounding terrain at sites A and B also were used to measure soil hydraulic properties. Bulk density ranged from 1.35 to 1.50 grams per cubic centimeter (g/cm^3), specific gravity ranged from 2.52 to 2.62, and the hydraulic conductivity ranged from 1.0 to 3.4 centimeters per day, which is consistent with the range in hydraulic conductivity for silty clays reported by Das (2009). The electrical conductivity of surface soil from the disposal fields and surrounding terrain at sites A and B was determined by using a method that involved a 1:2 fixed-volume, soil-to-water, direct measurement of soil electrical conductance. The electrical conductivity of soil from the disposal field at site B (1.0 decisiemens per meter) was approximately 35 percent greater than the electrical conductivity of the other locations tested (0.74 decisiemens per meter), likely because of the home water softener treatment system used by the residence at site B.

Table 2. Soil grain-size distribution and selected physical properties of soil samples collected from locations on the disposal fields and surrounding terrain at sites A and B.

[cm, centimeter; mm, millimeter; <, less than; g/cm^3, grams per cubic centimeter; cm/d, centimeters per day; EC, electrical conductivity; dS/m, decisiemens per meter; DF, disposal field; –, no data; ST, surrounding terrain]

Sample location	Sample depth below land surface (cm)	Percentage of sand[1] (0.05–2.0 mm)	Percentage of silt[1] (0.002–0.05 mm)	Percentage of clay[1] (<0.002 mm)	Textural classification[2]	Specific gravity[3] (unitless)	Bulk density[4] (g/cm^3)	Hydraulic conductivity[5] (cm/d)	$EC_{1:2}$ soil-to-water electrical conductivity[6] (dS/m)
				Site A					
DF	0–15.2	46	43	11	Loam	2.59	1.50	–	0.72
ST	0–15.2	51	27	22	Sandy clay loam	2.52	1.41	3.4	0.74
ST	15.2–30.5	38	34	28	Clay loam	2.61	1.35	1.8	–
ST	30.5–45.7	35	42	23	Loam	2.61	1.38	1.7	–
				Site B					
DF	0–15.2	42	40	18	Loam	2.62	1.43	–	1.0
ST	0–15.2	43	36	21	Sandy clay loam	2.59	1.41	1.3	0.76
ST	15.2–30.5	64	12	24	Sandy clay loam	2.59	1.43	1.1	–
ST	30.5–45.7	69	7	24	Loam	2.60	1.44	1.0	–

[1]Determined by using sieve and hydrometer methods that use the Unified Soil Classification System defined particle-size limits.

[2]Determined by using U.S. Department of Agriculture Textural Soil Classification.

[3]Determined by using U.S. Department of Agriculture Soil Texture Triangle Hydraulic Properties Calculator.

[4]Determined by using American Standard Test Method D854-10.

[5]Determined by using constant-head permeameter method.

[6]Determined by using 1:2 fixed volume soil-to-water electrical conductance direct measurement method.

The average distance from the soil surface to the top of bedrock at sites A and B was less than 2 m below land surface, determined by using a truck-mounted, direct-push, soil-probing machine (540UD, Geoprobe Systems, Salina, Kansas). The average depth to groundwater at sites A and B was approximately 48 m, on the basis of groundwater levels from plate 1 in Bartolino and others (2010) that shows a geohydrologic map of the East Mountain study area, central New Mexico.

Direct-push boreholes were completed to depths of 1.5 to 2 m below land surface in the disposal fields and in the surrounding terrain at site A on August 17, 2010, and at site B on August 18, 2010. Direct-push boreholes were completed midway between and near the distal end of the effluent-distribution lines in disposal fields; boreholes in the surrounding terrain were completed at a distance of several meters beyond the vegetated area that covers the disposal field and are assumed to be outside the influence of seepage from the distribution lines. Continuous soil core samples were collected from the boreholes with a 1.2-m-long, 5-cm-outer-diameter, steel, split-barrel sampler equipped with 2.54-cm-diameter, transparent, acetate barrel liners. At each borehole location, continuous soil cores were retrieved from the land surface to a depth where the split-barrel sampler could no longer be advanced by using the direct-push machine. This maximum penetration depth was assumed to be the depth to bedrock on the basis of highly weathered fragments of limestone observed in the sample cores retrieved from those depths. As the sample cores were retrieved, the sample-filled liner was sealed with a polypropylene cap, and samples were immediately chilled for transport to the USGS New Mexico Water Science Center sediment laboratory.

Volumetric soil-water content is expressed as the percentage of water by volume and calculated as the percentage of soil water by weight (weight loss in grams during oven drying at 101 °C for 24 hours) multiplied by the ratio of the bulk density of the soil (1.41 g/cm^3 for the disposal field and surrounding terrain at site A and 1.43 g/cm^3 for the disposal field and surrounding terrain at site B) to the density of water (1.00 g/cm^3). The volumetric soil-water content was determined for composited samples from the soil cores at sites A and B at depth intervals of 0.1 m (figs. 7*A–B*). The volumetric soil-water content data show that, in general, the upper and lower sections of the soil profiles were wetter than the middle sections, with the greatest volumetric soil-water content observed in the lower sections. As expected, soil from the disposal fields was wetter than soil from the surrounding terrain at sites A and B, and in general, the soil at site B was wetter than the soil at site A. A total of 38.9 mm of precipitation occurred in the 2 weeks preceding soil core sampling, with 17.0 of the 38.9 mm occurring in the early morning hours of August 18, 2010 (Weather Underground, 2013), which could explain the wet conditions observed in the upper sections of the soil profiles. The generally wetter conditions observed at site B compared to site A could be attributed to shading from the copse of trees near to where the soil cores were collected at site B.

Water-Budget Approach

A water budget accounts for all inputs to and outputs from a system and is based on the principals of the conservation of mass. Water budgets can be applied to hydrologic systems, such as a disposal field or the natural terrain surrounding a disposal field. In this study, a water-budget approach used values of known or measurable input and output components in a mass-balance equation to solve for the value of an unknown or unmeasured component. A detailed explanation of the water-budget approach as applied to a disposal field and the assumptions inherent when applying this technique can be found in Stannard and others (2010). The water budget for a disposal field can be written as follows:

$$P + Dose = ET_{DF} + D_{DF} + R_{DF} + \Delta S_{DF} \quad (1)$$

and for the surrounding terrain can be written as follows:

$$P = ET_{ST} + D_{ST} + R_{ST} + \Delta S_{ST} \quad (2)$$

where—during a specified period of time, over a given area, and in consistent units—

- P is precipitation,
- $Dose$ is the effluent delivered to the disposal field,
- ET is evapotranspiration,
- D is drainage,
- R is surface runoff, and
- ΔS is the change in soil-moisture storage, and where the subscripts DF and ST refer to the disposal field and the surrounding terrain, respectively.

These individual components are fluxes, and the mass-balance equation assumes that no appreciable lateral flow of effluent occurs to or from the disposal field into the surrounding terrain (Sherlock and others, 2002). If the contributions of surface runoff and the change in the soil-moisture storage to the mass-balance equation are negligible over sufficiently long times, as suggested in Stannard and others (2010), then the remaining components of the mass-balance equation are precipitation, dose, drainage, and ET. The amount of effluent dosed to a disposal field potentially available for groundwater recharge can be expressed as the difference between equation 1 and equation 2:

$$D_{DF} - D_{ST} = Dose - (ET_{DF} - ET_{ST}) \quad (3)$$

The precipitation terms in equations 1 and 2 cancel out in equation 3 because the amount of precipitation is assumed to be the same on the disposal field and on the surrounding terrain. The amount of drainage from a disposal field that is due to effluent can be determined as the amount of drainage on the disposal field (D_{DF}) less the amount of drainage on the surrounding terrain (D_{ST}). Similarly, the amount of ET from a disposal field that is due to effluent can be determined as the amount of ET on the disposal field (ET_{DF}) less the amount of

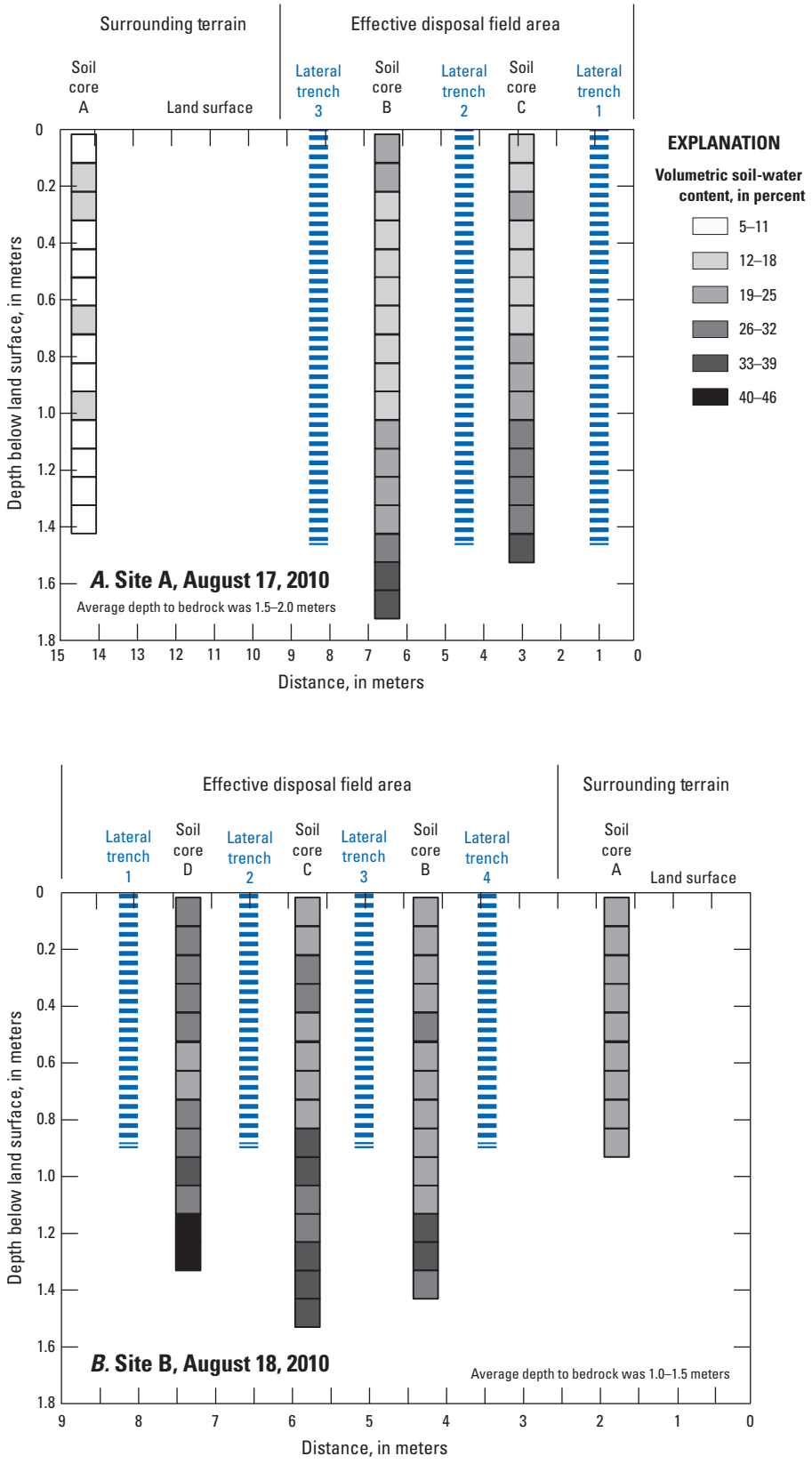

Figure 7. The percentage of volumetric soil-water content of core samples retrieved from the disposal field and the surrounding terrain at *A*, site A on August 17, 2010, and *B*, site B on August 18, 2010.

ET on the surrounding terrain (ET_{ST}). In this study, the amount of effluent dosed to a disposal field that is potentially available for recharge was computed as the mean daily volume of effluent dosed to the disposal field in excess of the mean daily volume of effluent loss from ET from the disposal field.

Data Collection and Methods of Effluent Dose Estimation

The daily volume of effluent dosed to the disposal fields was estimated by using the horizontal surface area of the septic tank multiplied by the total daily effluent-level change within the septic tank. At sites A and B, a vented 15-pounds-per-square-inch pressure transducer (Level Troll 500, In-Situ Inc., Fort Collins, Colo.) was installed in the secondary septic tank so that the depth of pressure-transducer submergence could be used to determine the change in effluent level in the septic tank resulting from the partial filling and partial emptying of the septic tank (fig. 4). Because effluent can be highly corrosive, the pressure transducers were housed inside an approximately 1.8-m-long section of PVC pipe that was perforated near the bottom to allow contact between the pressure transducer and the effluent in the septic tank. The submergence recorded by the pressure transducer was checked at each visit by using a steel tape; however, field measurements were only used to check the transducer function because only the relative change in the effluent level was used in the computation of dose volume. The submergence depth of the pressure transducer was recorded every 25 minutes (min), except when the absolute value of the change in effluent level was equal to or greater than 1.8 mm, and then data were recorded every 5 seconds (sec). Figure 8 shows the level of pressure-transducer submergence and the cumulative discharge of effluent from the secondary septic tank at site A on June 30, 2011. The changes in pressure-transducer submergence, which resulted from the accumulation and subsequent dosing of effluent, indicated that the pump in the septic tank was activated four times on that day.

The horizontal surface area of the septic tank, determined from schematics provided by Albuquerque Vault Company, was 4.9 m^2. The change in the depth of submergence recorded by the pressure transducer inside the septic tank, either positive (accumulation of effluent in the septic tank) or negative (dose of effluent from the septic tank), was computed for all consecutive submergence data recorded to identify

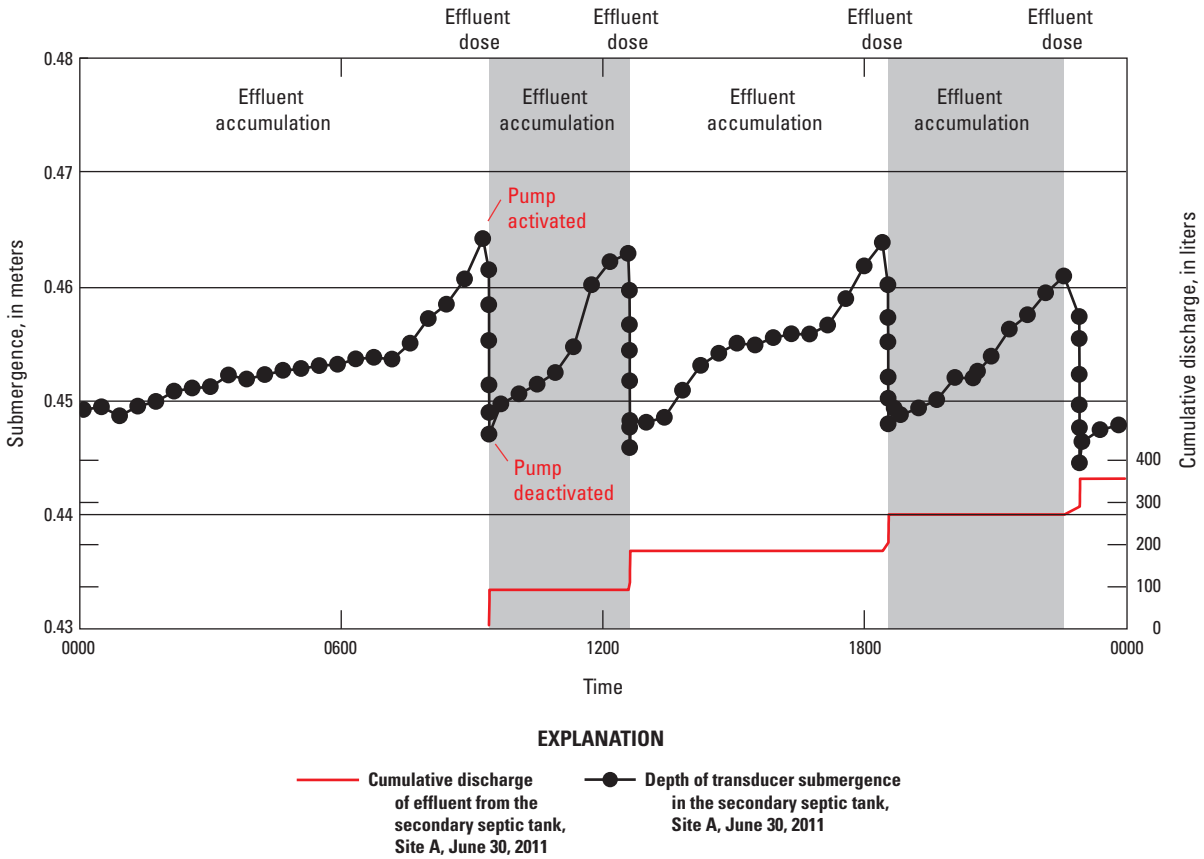

Figure 8. The changes in pressure-transducer submergence resulting from the accumulation and subsequent dosing of effluent, and the cumulative discharge of effluent from the secondary septic tank at site A over a 24-hour period on June 30, 2011.

pump cycles. The change in effluent level inside the septic tank during a pump cycle was determined as the difference between the maximum level of effluent in the septic tank before the pump cycle and the minimum level of effluent in the septic tank after the pump cycle. The volume of effluent pumped from the septic tank during a cycle was computed as the product of the horizontal surface area of the septic tank and the change in effluent level (height).

Uncertainties associated with the effluent volume computation include the small amount of effluent not accounted for if effluent enters the septic tank during a pump cycle, pressure-transducer accuracy (less than 0.003 m at 15 °C), and limitations in determining the true maximum and minimum submergence before the pump activation or deactivation. These uncertainties were estimated to be less than 1.9 liters per cycle, or 2 percent of the pumped volume per cycle. Submergence data used in the calculation of effluent dose volume for the septic tanks at sites A and B are archived and are available by request from the USGS New Mexico Water Science Center.

Data Collection and Methods of Evapotranspiration Estimation

Evapotranspiration is the quantity of water transferred to the atmosphere as water vapor from the ground surface by evaporation from soil and by transpiration from plants (Shuttleworth, 2008). Estimates of actual ET occurring from the land surface (actual ET) can be measured directly by using a flux chamber or modeled by using an energy-balance equation, such as the Penman-Monteith (PM) equation. Evapotranspiration varies with vegetation type and cover. Flux chambers are useful for measuring ET from locations with inadequate fetch, sparse or short canopies, or bare soil, such as can be found on a disposal field or the natural terrain in semiarid regions (Stannard, 1988).

In this study, ET loss from the disposal fields and the surrounding terrain at sites A and B was estimated by using modeled ET calibrated with periodic ET measurements. Data collected from micrometeorological and soil instrumentation on the disposal fields and on the surrounding terrain at sites A and B were used as input data into the PM equation to model continuous ET. Actual ET was measured periodically at fixed locations on the disposal fields and on the surrounding terrain by using a portable hemispherical flux chamber (ET chamber). Field measurements of actual ET were conducted throughout the year and at various times of the day to capture the seasonal and daily variability in ET rates at the fixed locations. Actual ET data determined from ET chamber measurements were used to calibrate PM model estimations of ET.

Micrometeorological and Soil-Data Collection

Micrometeorological and soil data were collected at sites A and B (figs. 3 and 5) for use as input data into the PM equation. Micrometeorological stations located on the surrounding terrain at each site measured precipitation, barometric pressure, air temperature, relative humidity, wind speed, and wind direction. Soil and net radiation instrumentation were installed on the disposal fields and on the surrounding terrain at each site and included measurements of soil temperature, soil heat flux, volumetric soil-water content, and net radiation. The placement of the micrometeorological stations was selected in consideration of wind direction, physical barriers, sun angle, and shadows. The placement of soil and net radiation instrumentation was selected to best approximate the average hydrologic conditions on the disposal fields and on the surrounding terrain, given limited equipment and resources. Upwind fetch is the horizontal distance between the location of micrometeorological measurements (micrometeorological station) and a change in surface conditions (edge of the disposal field) in the direction of prevailing winds (northwest to northeast during the study). Although disposal fields were within the upwind fetch of micrometeorological stations, they were assumed to have no influence on micrometeorological measurements given the relatively small size of the disposal field areas (Stannard, 1997; Berger and others, 2001).

At site A, micrometeorological instrumentation was mounted on a 3-m-tall aluminum tower installed approximately 4 m east of the disposal field (fig. 3*A*). Soil and net radiation instrumentation at site A were installed at fixed locations on the disposal field and on the surrounding terrain, with the optical sensor of the net radiometer located above the subsurface soil instruments. On the disposal field, soil instruments were installed approximately one-quarter of the way between two effluent-distribution lines—lateral 1 and lateral 2—such that measurements collected from this location might best represent the average hydrologic conditions of the disposal field (fig. 5*A*). On the surrounding terrain, soil instruments were installed approximately 2 m east of the micrometeorological station.

At site B, micrometeorological instrumentation was mounted on a 3-m-tall aluminum tower installed on the surrounding terrain at a location that was approximately 18 m west of the disposal field (fig. 3*B*). Soil and net radiation instrumentation at site B were installed at fixed locations on the disposal field and on the surrounding terrain, with the optical sensor of the net radiometer located above the subsurface soil instruments (fig. 5*B*). On the disposal field, soil instruments were installed approximately one-quarter of the way between two effluent-distribution lines—lateral 3 and lateral 4—such that measurements collected from this location might best represent the average hydrologic conditions on the disposal field. On the surrounding terrain, soil instruments were installed approximately 2 m south of the micrometeorological station.

Micrometeorological and soil data were collected at site A from January 1, 2011, to December 31, 2012, and at site B from February 24, 2011, to December 31, 2011; all data are compiled in appendix 1. Data were recorded by using

a data logger (model CR1000, Campbell Scientific, Inc., Logan, Utah) powered by a 12-volt, 18-ampere hour battery. From January 2011 to August 2011, data were measured once per minute and aggregated into 15-min mean values, except for precipitation data, which were summed every 15 min, and soil temperature data, for which only the final value for every 15-min period was used. From August 2011 to December 2012, data were measured once every 10 sec and aggregated into 15-min mean values, except for precipitation data, which were summed every 15 min, and soil temperature data, for which only the final value for every 15-min period was used. All data were recorded in Coordinated Universal Time (UTC) and were later converted to Mountain Daylight Time (MDT). The micrometeorological instrumentation installed at sites A and B included a combined air temperature and relative humidity probe (model HMP45C, Vaisala, Inc., Woburn, Massachusetts) housed inside a naturally aspirated, 10-plate, gill radiation shield (model 41003, R.M. Young Co., Traverse City, Michigan), a tipping-bucket rain gage (model TE525WS, Texas Electronics, Inc., Dallas, Tex.) with a snowfall adapter (model CS705, Campbell Scientific, Logan, Utah) used during the winter, a barometric pressure sensor (model 278, Setra Systems, Inc., Boxborough, Mass.), and a wind speed and wind direction monitor (site A, model 05103, R.M. Young Co., Traverse City, Mich.; site B, models 014A and 024A, Met One Instruments, Rowlett, Tex.). Net radiometers (model NR-Lite2, Kipp & Zonen USA, Inc., Bohemia, New York) at sites A and B were installed at a height (1.04 m at site A and 0.91 m at site B) to minimize the amount of source area captured by the sensor from outside of the target area, and net radiation data were corrected for wind speed in excess of 5 m/s by using methods outlined in Campbell Scientific, Inc. (1998). Soil instrumentation for both locations at sites A and B included a soil heat flux plate (model HFP01, Hukseflux USA, Inc., Manorville, N.Y.) installed 8 cm below land surface; averaging soil temperature probes (model TCAV, Campbell Scientific, Inc., Logan, Utah) with two temperature probes installed at 2 and 6 cm below land surface, respectively; and a soil-water content probe (CS616, Campbell Scientific, Inc., Logan, Utah) installed from 2.5 to 5.5 cm below land surface. Subsurface soil instrumentation at sites A and B were installed by following instructions for the installation of a Bowen-ratio station outlined in Campbell Scientific, Inc. (1987). Instruments were tested prior to deployment and checked for proper function during each site visit. Instrument-specific calibration constants (from manufacturer calibration certificates) were applied where appropriate in data-logger programs to convert voltages into desired units of measure.

The soil-water content probes used in this study operate on time domain reflectometry (TDR) technology, which assumes a negligible loss of apparent dielectric permittivity—an assumption that can be invalid in soils with high electrical conductivity, such as clay or saline soils (Bittelli and others, 2008). Dielectric losses caused by conductive soils can result in a soil-water content measurement that overestimates soil-water content. Overestimation of soil-water content can be avoided by using a soil-specific calibration curve from measurements of volumetric soil-water content (product of gravimetric soil-water content and bulk density). Calibration curves for the TDRs used in this study were determined from laboratory-derived measurements of volumetric soil-water content of representative soil samples from the disposal fields and surrounding terrain at sites A and B over a range of values (dry to fully saturated) by following methods outlined in Campbell Scientific, Inc. (2002a). Fractional volumetric soil-water content data, calibrated to soil-specific measurements, are provided in appendix 1.

Uncertainties associated with the collection of micrometeorological and soil data include instrument accuracy and response time, instrument calibration drift, and the uncertainty of using a single value of a parameter to represent the average value of that parameter in a system where field properties can be spatially variable. Where possible, instruments with high sensor accuracy and rapid response times were selected for this study. The calibration drift of an instrument was evaluated by either comparison of the value to values reported at other sites nearby or comparison of the value to values determined by using independent field methods. The uncertainty associated with choosing a representative sample location was reduced by using field measurements and observations to determine a location most representative of the average hydrologic conditions.

Evapotranspiration Chamber Data Collection

Field measurements of actual ET were collected at fixed locations on the disposal field and on the surrounding terrain at site A during 2011−12 and at site B during 2011 by using an ET chamber. The ET chamber is a Plexiglas dome approximately 1 m in diameter that is equipped with two opposing variable-speed fans mounted on the interior dome wall and a combined air temperature and relative humidity probe (fig. 9) (Stannard, 1988). At site A, ET chamber measurements were collected at 9 fixed locations along a cross section that included 5 locations on the disposal field and 4 locations on the surrounding terrain (fig. 5*A*). At site B, ET chamber measurements were collected at 11 fixed locations along a cross section that included 7 locations on the disposal field and 4 locations on the surrounding terrain (fig. 5*B*). Measurement locations on the disposal fields included locations above and between the effluent-distribution lines to capture the spatial heterogeneity in ET across the disposal field. Measurement locations on the surrounding terrain were selected several meters from the vegetative growth on the disposal fields at a distance far enough from the disposal field that would not be affected by effluent dosed to the outer effluent-distribution lines.

Discrete ET chamber measurements were collected at fixed locations along the established cross sections at sites A and B, with measurements lasting about 2 min per fixed location by following procedures outlined in Stannard (1988). Cross-section measurements were repeated every

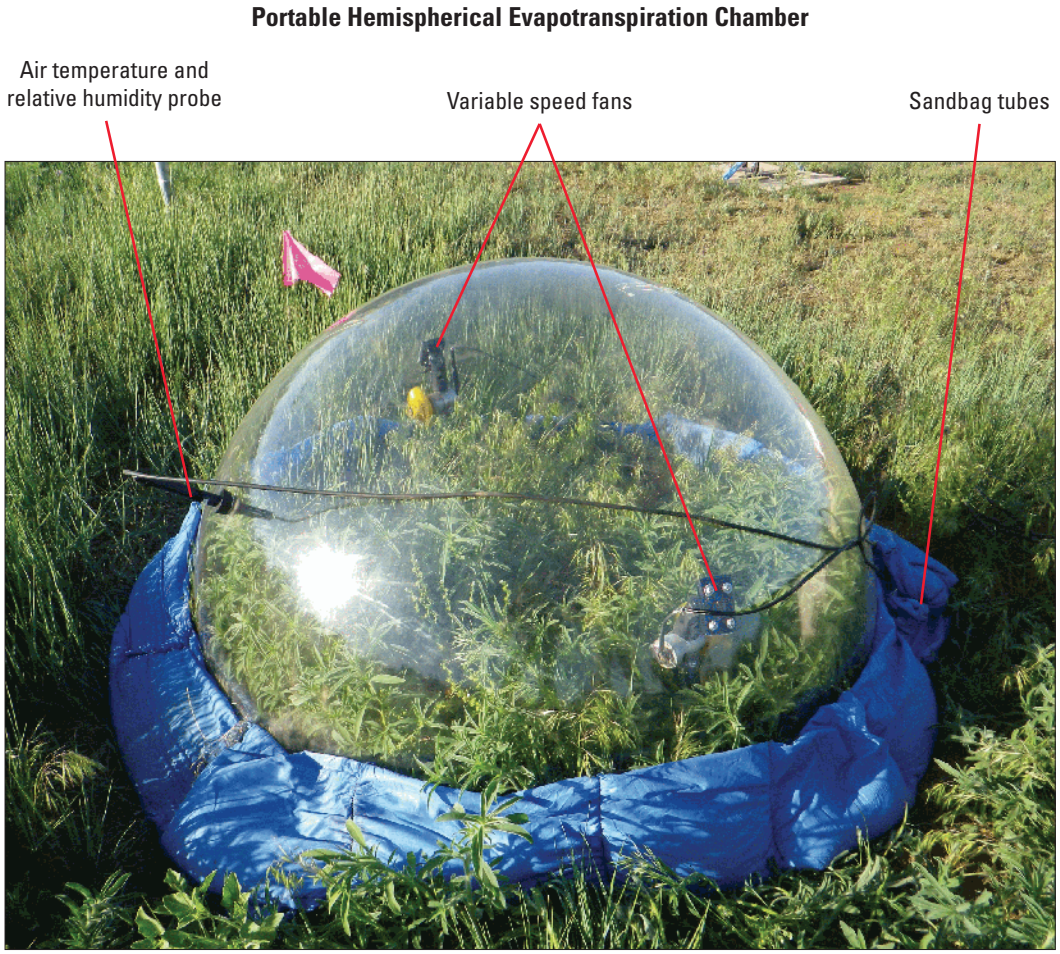

Figure 9. Measurement of actual evapotranspiration by using a portable hemispherical evapotranspiration chamber on the disposal field at site A on May 19, 2012.

30 min, when possible, throughout the day to capture temporal variability in ET (table 3). Prior to each ET chamber measurement, the mean wind speed was measured in the field by using a hand-held anemometer, and a voltage-to-wind speed correlation was used to adjust the speed of the fans inside the ET chamber to approximate the mean wind speed measured outside of the ET chamber. On windless days, a minimum threshold of 0.32 m/s was used to provide sufficient air mixing inside the ET chamber. At the onset of each measurement, the ET chamber was placed over the measurement location with care to not flatten any vegetation in the process. To create a seal between the base of the ET chamber and the sometimes uneven land surface, three sandbag tubes (10-cm-wide and 1.55-m-long nylon fabric tubes filled with play sand) were used to block air gaps (fig. 9). The sandbag tubes were also found to function well in reducing the amount of dust that was statically attracted to the ET chamber during measurements, which could affect measurements by interfering with light transmission. During each ET chamber measurement, the air temperature and relative humidity were measured every 2 sec inside the ET chamber by using a high-accuracy rapid-response probe (HydroClip S, Rotronic Instrument Corp., Hauppauge, N.Y.). Following each measurement, the ET chamber was lifted for approximately 30 sec to purge any saturated air accumulated inside the ET chamber during the prior test and to allow the ET chamber to equilibrate with the ambient conditions before beginning the next measurement.

Data from the combined air temperature and relative humidity probe inside the ET chamber were used to compute vapor density by using the following equation:

$$D_v = \frac{RH * e_s}{T * 4.6153 * 10^{-4}} \quad (4)$$

where

D_v is vapor density, in grams per cubic meter;
RH is relative humidity (unitless);
e_s is saturation vapor pressure, in kilopascals;
T is air temperature, in Kelvins; and
$4.6153*10^{-4}$ is the gas constant for water vapor, in kilopascal cubic meter per grams Kelvins.

Table 3. Summary of the date, duration, and total number of evapotranspiration chamber measurements collected on the disposal fields and on the surrounding terrain at sites A and B during 2011–12.

[ET, evapotranspiration; MDT, mountain daylight time; DF, disposal field; ST, surrounding terrain]

Date of ET chamber measurement	Time of day during data collection (MDT)[1]	Number of ET chamber measurements conducted on DF during data collection	Number of ET chamber measurements conducted on ST during data collection
	Site A		
June 1, 2011	1330 to 1400	1	2
June 28, 2011	1115 to 1300	6	2
September 14, 2011	1245 to 1500	25	14
September 21, 2011	1000 to 1300	30	14
November 30, 2011	1430 to 1600	15	14
May 19, 2012	1815 to 2000	15	12
June 14, 2012	1130 to 1515	20	18
June 15, 2012	1045 to 1215	10	8
July 14, 2012	1745 to 1945	15	12
July 15, 2012	0615 to 0700	10	8
September 15, 2012	1815 to 1900	5	4
September 16, 2012	0715 to 0845	10	8
	Site B		
June 10, 2011	1145 to 1315	2	1
September 16, 2011	1000 to 1230	35	11
November 30, 2011	1215 to 1345	21	12

[1]Time of day was rounded to 15-minute intervals.

Saturation vapor pressure was estimated as a function of air temperature by using the empirical relation of Lowe (1977). The time series of computed vapor density during a measurement was plotted to determine the maximum rate of change in vapor density inside the ET chamber (fig. 10). The maximum rate of change in vapor density inside the ET chamber was determined as the steepest slope of the vapor density time series on the basis of an 11-point moving-slope calculation (fig. 10). The maximum slope of the vapor density time series was then used to determine the rate of ET during the ET chamber measurements by using the following equation:

$$ET = 86.4\left(\frac{M_{max} * V * C}{A}\right) \quad (5)$$

where

ET is evapotranspiration, in millimeters per day;
M_{max} is the steepest 11-point slope section of the vapor density time series, in grams per cubic meter per second;
V is the volume inside the ET chamber, in cubic meters;
C is the calibration constant of the ET chamber (unitless);
A is the area of surface encompassed by the ET chamber, in square meters; and
86.4 is the conversion factor that converts grams of water per square meter per second to millimeters of water per day.

The volume of the ET chamber used in this study was 0.245 cubic meters (m^3), and the calibration constant was 1.03 (unitless). The ET chamber calibration constant—used to account for Plexiglas water-vapor adsorption, sensor error, and incomplete air mixing inside the ET chamber—was determined by Jason Masoner and Kevin Smith from the USGS Oklahoma Water Science Center by using a weighted water-loss calibration technique outlined by Stannard (1988).

Penman-Monteith Model Estimation of Evapotranspiration

The PM equation is an ET model based on energy-balance and mass transfer where latent heat flux is the amount of ET expressed as an energy flux. The PM equation represents the energy balance of an evaporating surface as a single "big leaf," where a single surface conductance

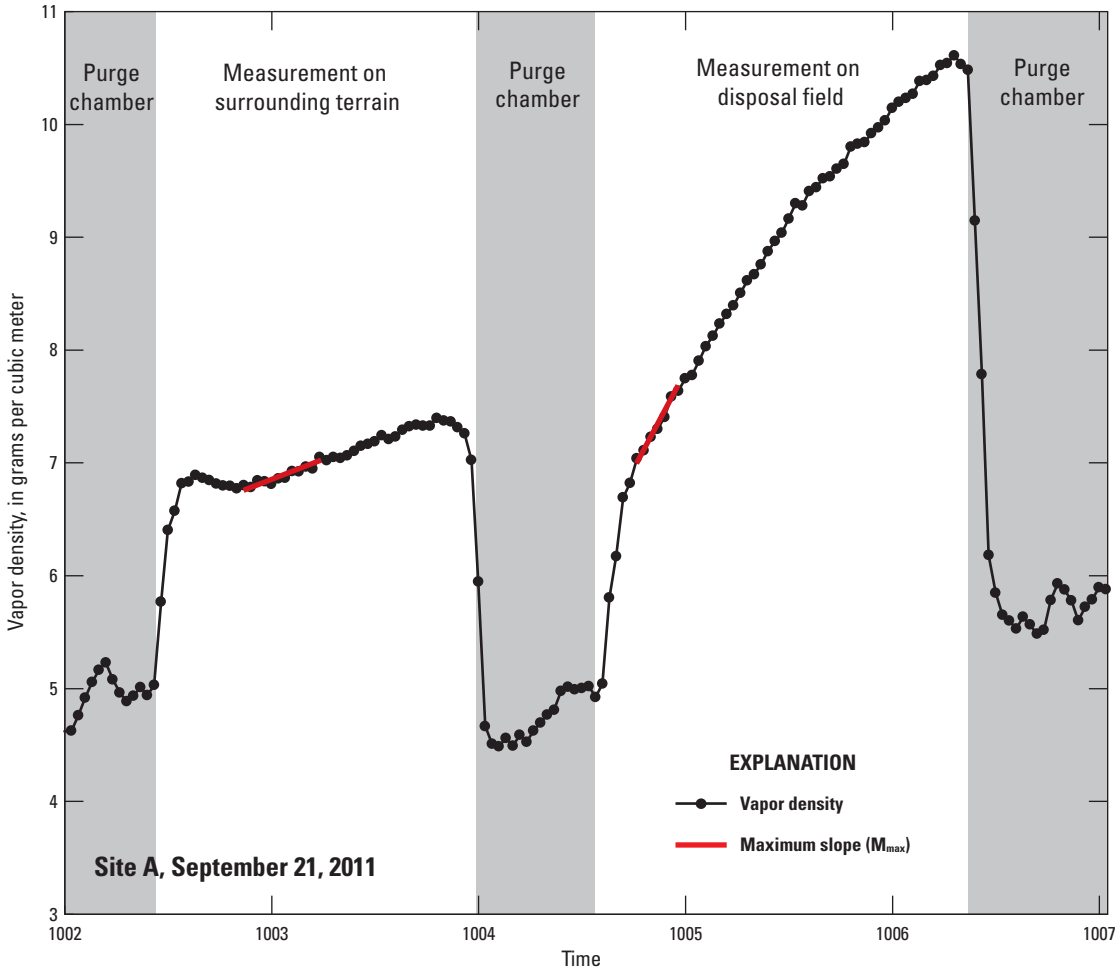

Figure 10. Vapor density inside the evapotranspiration chamber and the maximum slope of the vapor density curve during the data collection period at site A on September 21, 2011.

term and a single aerodynamic conductance term represent the mass transfer properties of the evaporating surface and overlying air. The form of the PM equation used in this study follows Stannard and others (2010) and can be written as follows:

$$\lambda E = \frac{\Delta\left(R_n - G\right) + g_a \rho C_p VPD}{\Delta + \gamma\left(1 + \frac{g_a}{g_c}\right)} \quad (6)$$

where

λE is the latent heat flux, in watts per square meter;

Δ is the slope of the saturation vapor pressure curve, in kilopascals per degree Celsius;

R_n is net radiation, in watts per square meter;

G is soil heat flux, in watts per square meter;

g_a is aerodynamic conductance, in meters per second;

ρ is air density, in kilograms per cubic meter;

C_p is the specific heat of air, in joules per kilogram per degree Celsius;

VPD is the vapor pressure deficit of air, in kilopascals;

γ is the psychrometric constant, in kilopascals per degree Celsius; and

g_c is canopy conductance, in meters per second.

Latent heat flux can be expressed as ET in millimeters per day (mm/d) by using a conversion factor of 0.0353, where 1 mm/d of ET is equal to 2.45 megajoules per square meter per day. The terms Δ, g_a, ρ, γ, and VPD used in the PM equation were estimated by using the methods described in Allen and others (2005) and Stannard and others (2010). The terms R_n and G are field-measured values, with G being soil heat flux at land surface determined through equations described in Campbell Scientific, Inc. (2002b). The specific heat of dry air at constant pressure (C_p) is 1,004 joules per kilogram per degree Celsius,

and the term for canopy conductance (g_c) can be determined as follows:

$$g_c = \begin{cases} g_s * LAI + g_e, \ if \ g_e \geq g_s * LAI \\ g_s * LAI, otherwise \end{cases} \quad (7)$$

where

g_c is canopy conductance, in meters per second;
g_s is stomatal conductance, in meters per second;
LAI is the green leaf area index (unitless); and
g_e is soil surface conductance, in meters per second.

The addition of soil surface conductance (g_c) only occurs when g_c is greater than the product of stomatal conductance (g_s) and LAI, which typically happens at night or during the non-growing season when vegetative cover is dormant or sparse. The term g_c is discussed later in this section (see equation 9a). The LAI term in this study was estimated by using a two-color interpretation of photographs combined with a vegetation grid counting technique in a method modified from Monteith and Unsworth (1990). This method, which was different from the method used by Stannard and others (2010), was adopted to better estimate LAI for a sparsely-vegetated landscape (see "Leaf Area Index Data Collection and Estimation" section).

Stomatal conductance (g_s) is a difficult variable to measure and, as such, can be related to more easily measured variables that are assumed to influence g_s such as net radiation, volumetric soil-water content, vapor pressure deficit, and time of day (Stannard and others, 2010). Stomatal conductance (g_s) was modeled by using the following equation:

$$g_s = g_{smax} * f[R_n] * f[\theta] * f[VPD] * f[t] \quad (8a)$$

where

g_s is stomatal conductance, in meters per second;
g_{smax} is the maximum value of g_s, in meters per second;
f is an influence function from 0 to 1 (unitless);
θ is volumetric soil-water content, in cubic centimeters of water per cubic centimeters of soil;
t is time, in decimal hours; and
R_n and VPD are as previously defined in equation 6.

The influence functions for net radiation, volumetric soil-water content, vapor pressure deficit, and time of day were used to determine g_s by following Stannard and others (2010). The influence function for net radiation was determined as follows:

$$f[R_n] = \frac{(R_n - K)(R_{nmax} - K + C_1)}{(R_{nmax} - K)(R_n - K + C_1)} \quad (8b)$$

where

$f[R_n]$ is the modeled influence of net radiation from 0 to 1 (unitless);
R_n is the net radiation, in watts per square meter;
K is the value of net radiation as solar radiation goes to zero, in watts per square meter;
R_{nmax} is the maximum net radiation, in watts per square meter; and
C_1 is a modeled parameter determined by nonlinear regression (unitless).

At site A, the maximum R_n values were 785 and 685 watts per square meter for the disposal field and the surrounding terrain, respectively (table 4). At site B, the maximum R_n values were 709 and 730 watts per square meter for the disposal field and the surrounding terrain, respectively. The value of K for all locations was -62 watts per square meter, determined as the average value of R_n at sites A and B when entering astronomical twilight. The influence function for volumetric soil-water content was determined as follows:

$$f[\theta] = \frac{1 - \exp(C_2 \times \theta_E)}{1 - \exp(C_2)} \quad (8c)$$

where

$f[\theta]$ is the modeled influence of volumetric soil-water content from 0 to 1 (unitless);
exp() is the exponential function (dimensionless);
C_2 is a modeled parameter determined by nonlinear regression (unitless); and
θ_E is the value of volumetric soil-water content available to plants, in cubic centimeters of water per cubic centimeters of soil.

The value of volumetric soil-water content available to plants (θ_E) was determined as follows:

$$\theta_E = \frac{\theta - \theta_{wp}}{\theta_{fc} - \theta_{wp}} \quad (8d)$$

where

θ_E is the volumetric soil-water content available to plants, in cubic centimeters of water per cubic centimeters of soil;
θ is the volumetric soil-water content value, in cubic centimeters of water per cubic centimeters of soil;
θ_{fc} is the value of volumetric soil-water content at field capacity, in cubic centimeters of water per cubic centimeters of soil; and
θ_{wp} is the value of volumetric soil-water content at the wilting point of 0.097, in cubic centimeters of water per cubic centimeters of soil.

The value of volumetric soil-water content at field capacity—the amount of volumetric soil-water content held in the soil after excess water has drained away—was determined by using an approach similar to Stannard and others (2010). The average volumetric soil-water content value at field capacity on the disposal field at sites A and B was 0.331 cubic

Table 4. Value of parameters associated with the Penman-Monteith equation used to model evapotranspiration on the disposal fields and on the surrounding terrain at sites A and B during 2011–12.

[Parameters are reported for both site A and B except where indicated otherwise. m/s, meter per second; VPD, vapor pressure deficit; W/m^2, Watts per square meter; m, meter; kg/m^3, kilograms per cubic meter]

Description of parameter	Parameter	Disposal field	Surrounding terrain
Model input parameters			
Maximum stomatal conductance	$g_{s\text{-}max}$ (m/s)	7.25E^{-3}	4.90E^{-4}
Maximum surface conductance corresponding to soil evaporation	$g_{e\text{-}max}$ (m/s)	2.10E^{-3}	1.10E^{-3}
Model parameter for net radiation influence function	C_1 (unitless)	1	1
Model parameter for soil water content influence function	C_2 (unitless)	-1.74	0.81
Model parameter for VPD influence function	C_3 (unitless)	-0.76	-0.76
Model parameter for time of day influence function	C_4 (unitless)	0.012	0.012
Model parameter for time of day influence function	C_5 (unitless)	14	14
Model parameter for soil evaporation influence function	C_6 (unitless)	-0.46	-0.34
Maximum net radiation, site A	$R_{n\text{-}max}$ site A (W/m^2)	785	685
Maximum net radiation, site B	$R_{n\text{-}max}$ site B (W/m^2)	709	730
Mean value of R_n as R_s approaches zero	K (W/m^2)	-61	-63
Surface roughness length, site A (Hansen, 1993)	Z_{mf} site A (m)	0.3	0.3
Surface roughness length, site A (Hansen, 1993)	Z_{mf} site B (m)	1.2	1.2
Wind speed sensor height, site A	Z_w site A (m)	2.84	2.84
Wind speed sensor height, site B	Z_w site B (m)	2.26	2.26
Vegetation height	h_c (m)	0.566	0.055
Average bulk density of soil	ρb (kg/m^3)	1,480	1,400
Model result parameters			
Coefficient of efficiency (Nash and Sutcliffe, 1970)	CE	0.79	0.37
Coefficient of determination	R^2	0.79	0.45
Root-mean-squared error of modeled value	RMSE (W/m^2)	35.7	13.6

centimeters (cm^3) of water per cubic centimeters of soil and the average volumetric soil-water content value at field capacity on the surrounding terrain at sites A and B was 0.281 cm^3 of water per cubic centimeters of soil. The influence function for vapor pressure deficit was determined as follows:

$$f[VPD] = \exp(C_3 * VPD) \quad (8e)$$

where

$f[VPD]$ is the modeled influence of VPD from 0 to 1 (unitless),

VPD is as previously defined,

exp() is the exponential function (dimensionless), and

C_3 is a modeled parameter determined by nonlinear regression (unitless).

Lastly, the influence function for time of day was determined as follows:

$$f[t] = 1 - C_4 (t - C_5)^2 \quad (8f)$$

where

$f[t]$ is the modeled influence of time of day from 0 to 1 (unitless), and

C_4, C_5 are modeled parameters determined by inspection, in hours squared and hours, respectively.

During periods of negligible canopy conductance, such as at night or during the non-growing season when vegetative cover is dormant or sparse, Stannard and others (2010, p. 342) used a method that estimated soil surface conductance (g_e) as "an overlying canopy of dormant grass" that was calibrated by

using chamber measurements from one non-growing season day; however, a different method was needed for this study, which had a sparsely vegetated landscape and used chamber measurements from several vegetation-free areas during growing and non-growing season days during 2012. For this study, a new method was developed to address periods when stomatal conductance was negligible—during the night and when LAI approached or was equal to zero—an influence function representing soil surface conductance (g_e) was used to represent the contribution of soil evaporation (θ_e) to canopy conductance (eq. 7) and was defined as follows:

$$g_e = g_{emax} * f\left[\theta_e\right] \tag{9a}$$

$$f\left[\theta_e\right] = \frac{\theta\left(\theta_{fc} + C_6\right)}{\theta_{fc}\left(\theta + C_6\right)} \tag{9b}$$

where

g_e is soil surface conductance, in meters per second;

g_{emax} is the maximum value of g_e, in meters per second;

$f[\theta_e]$ is the modeled influence of soil surface conductance from 0 to 1 (unitless);

θ is the volumetric soil-water content for each site, in cubic centimeters of water per cubic centimeters of soil;

θ_{fc} is the value of volumetric soil-water content at field capacity for each site, in cubic centimeters of water per cubic centimeters of soil; and

C_6 is the modeled parameter determined by nonlinear regression (unitless).

The influence function for soil surface conductance was set to one when values of volumetric soil-water content were greater than field capacity and set to zero when the soil was frozen. The PM model utilized values of canopy conductance in estimating ET when canopy conductance was greater than soil surface conductance (typically during the day and at substantial vegetation density). When the soil surface conductance was greater than the canopy conductance (typically during the night and at low vegetation density), the PM model used a variation of the canopy conductance equation that included the addition of soil surface conductance in the estimation of ET. This method was created and used in order to capture the small influence canopy conductance had on the sparsely vegetated surrounding terrain.

In order to determine the contribution of soil evaporation in measurements of actual ET on the surrounding terrain, a section of the surrounding terrain at site A was sprayed with an herbicide and kept free of vegetation throughout 2012. Soil evaporation was measured at this vegetation-free area by using the ET chamber during each cross-sectional measurement. On average, soil evaporation accounted for 64 percent of the ET measured on the surrounding terrain on the basis of a comparison of ET chamber measurements on the vegetated and vegetation-free areas of the surrounding terrain during 2012.

The coefficients in the influence functions for R_n, θ, VPD, and g_e were determined through the use of multiple-variable nonlinear regression (Helsel and Hirsch, 2002), in which the maximum stomatal conductance (g_{smax}) for each regression analysis was modified in the direction of least standard error from the previous analysis until a minimum standard error was determined. Once the maximum stomatal conductance was determined, the value for the maximum soil surface conductance (g_{emax}) was determined through the same steps used in determining maximum stomatal conductance. The determination of maximum stomatal conductance and maximum soil surface conductance was an iterative process, with each iterative step narrowing down the final values of maximum stomatal conductance and maximum soil surface conductance.

Uncertainties in the model-estimated ET include random and systematic errors associated with micrometeorological and soil data, as well as errors intrinsic to the model itself, such as uncertainty in the numerical assumptions and coefficients used. The uncertainty in modeled ET is decreased with increased confidence in the influence functions used to calibrate the model. Confidence in the influence functions is increased with greater ET measurement frequency and with greater range in ET measurement conditions. The accuracy of the PM-modeled ET values was evaluated by comparing values of actual ET field measurements to values of ET predicted by the model. The goodness of fit between measured and modeled values was assessed by using the coefficient of efficiency (CE) (Nash and Sutcliffe, 1970), defined as follows:

$$CE = 1 - \frac{\Sigma\left(x - y\right)^2}{\Sigma\left(y - \bar{y}\right)^2} \tag{10}$$

where

CE is the coefficient of efficiency (unitless);

x is the modeled value of evapotranspiration, in millimeters per day; and

y is the measured value of evapotranspiration, in millimeters per day.

The values of CE can range from negative infinity to one, with values closer to one indicating a higher correlation and goodness of fit between measured and modeled ET. According to Stannard and others (2010), in a modeling context, CE is a more stringent test of model performance as compared to the coefficient of determination (R^2).

Leaf Area Index Data Collection and Estimation

Leaf Area Index (LAI) is defined as the one-sided green leaf area per ground surface area. It is typically a difficult parameter to measure that also exerts strong influence on PM model results. For this study, LAI was determined by using a two-color (green and brown) photograph classification approach. Appendix 2 provides a description of the photograph locations and a summary of the data used to compute LAI. Photographs were taken at ET chamber measurement locations at sites A and B throughout the growing season of 2011 and 2012 by using a 35-mm digital camera tilted 30 degrees below horizontal. To avoid interference from shadows, photographs were consistently taken looking northward. Photographs were gridded with each cell of the grid classified as green or brown on the basis of the predominant pixel color observed: green pixels were interpreted as transpiring vegetation, and brown pixels were interpreted as dead and (or) dormant vegetation or bare soil. In some cases, the contrast or saturation of the photographs was manipulated to better differentiate the green pixels from the brown pixels. Leaf Area Index was computed as the negative natural logarithm of one minus the ratio of the number of grid cells with predominantly green pixels per total number of grid cells in a method modified from Monteith and Unsworth (1990). During each site visit, multiple photographs were taken of the disposal field and surrounding terrain. These photographs were used to determine a daily mean LAI for the disposal field and for the surrounding terrain. Leaf Area Index curves (best fit parabolic curves) were created from the daily mean LAI estimates from sites A and B for the disposal field and surrounding terrain (fig. 11). The same LAI curves for the disposal field and surrounding terrain was used for both years at both sites. The start and end dates of the growing season were defined for this study as March 15 and November 15, respectively, on the basis of field observations and information about western wheatgrass growing conditions. The LAI curves developed for this study are bimodal and are greater than the single-mode LAI curve reported by Stannard (1993) for semiarid rangeland (fig. 11).

Effective Drainage Area Estimation

In Stannard and others (2010), the effective drainage area of the disposal field was estimated as 35.7 m^2, an estimate that was based on the size of drain field required to support a

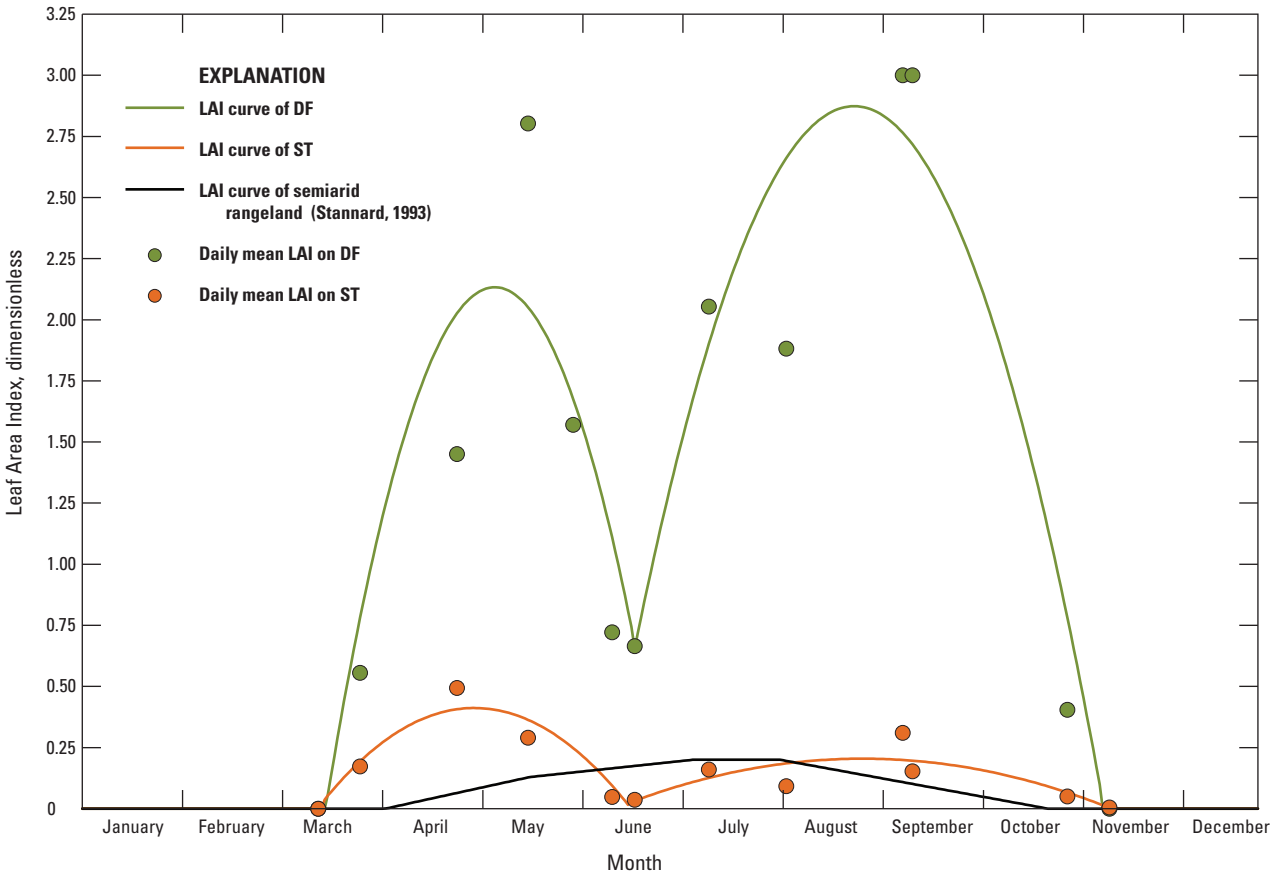

Figure 11. Leaf Area Index (LAI) curves smoothed to fit daily mean LAI measurements on the disposal field (DF) and the surrounding terrain (ST) for this study and the LAI curve of an arid rangeland reported by Stannard (1993).

two-bedroom household and a family of four. This estimate was used because the disposal field physical location was unknown and could not be easily differentiated from the surrounding terrain by greener or denser vegetation.

In this study, the physical dimensions of the disposal field (the length and width of the perimeter formed by the effluent-distribution lines) were known and used to define an effluent-drainage area of 117.1 m^2 and 89.7 m^2 at sites A and B, respectively; however, the effective effluent-drainage area at both sites was assumed to be slightly larger because of lateral seepage perpendicular to the effluent-distribution lines, as indicated by the vegetation density. The vegetation density indicated that not much seepage occurred outward from the distal ends of the effluent-distribution lines. The extent of lateral seepage perpendicular to the effluent-distribution lines was investigated on September 14, 2011, at site A and September 16, 2011, at site B by using ET chamber measurements collected at 0.91-m increments away from the edge of the disposal field. In general, the ET measured on the surrounding terrain decreased with distance from the edge of the effluent-distribution line. At a distance of 0.91 m from the edge of the disposal field, the measured ET was similar to that measured between the effluent-distribution lines on the disposal field, and at distances greater than 0.91 m, the measured ET was less than that measured anywhere on the disposal field. To account for lateral seepage perpendicular to the effluent-distribution lines, a total distance of 1.8 m was added to the width of the disposal field at sites A and B and multiplied by the length of the disposal field to best approximate an effective effluent-drainage area of 150.6 m^2 and 117.1 m^2, respectively.

Data Quality Assurance and Quality Control

Various types of quality assurance and quality control (QA/QC) methods were used in this study. Where possible, routine field maintenance activities such as sensor cleaning and inspection, verification of sensor performance against a known standard, and corroboration of data were performed. The quality of continuous micrometeorological data was assured by visual examination of the raw data, by comparison with independent field measurements collected during site visits by using a calibrated, portable weather meter (model 4500, Kestrel Meters, Birmingham, Mich.), by comparison of datasets from sites A and B to each other, and by comparison to micrometeorological data reported by personal weather stations KNMEDGEW7 (Weather Underground, 2012) and KNMTIJER2 (Weather Underground, 2013), located at or near the field sites. The quality of continuous TDR soil data was assured by visual examination of the raw data, by comparison with independent soil samples collected near the TDR sensor and analyzed for soil-water content in the laboratory, by comparison of datasets from sites A and B to each other, and by comparison to micrometeorological data collected at the field sites as part of this study, such as precipitation and soil temperature. The quality of continuous ET chamber data (air temperature and relative humidity) was assured by visual examination of the raw data, by comparison with independent field measurements collected by using a calibrated, portable weather meter (model 4500, Kestrel Meters, Birmingham, Mich.), and by sequential replicate measurements collected consecutively at a single sampling point location. The quality of continuous submergence data was assured by visual examination of the raw data, by periodic testing of sensor function, and by comparison of the computed effluent dose volume to an independent computed effluent dose volume recorded by a remote monitoring and control telemetry system (VeriComm, Orenco Systems, Inc., Sutherlin, Oreg.) installed in the secondary septic tank at sites A and B. All continuous data collected as part of this study are archived and are available by request from the USGS New Mexico Water Science Center.

Estimates of Potential Groundwater Recharge from Two Domestic Sewage Disposal Fields

A semiarid climate includes a complex mosaic of land-cover types, each of which may have differing ET rates. Although many factors can affect the amount of effluent storage and loss from a disposal field, no approach to ET or recharge estimation can fully capture the local-scale, spatial, and temporal variability in hydrogeologic and surficial conditions, which can affect the recharge rates. This assessment provides a best estimate of potential recharge from domestic disposal fields with low-pressure dosed sewage disposal systems in semiarid climates.

Estimated Effluent Dose

The submergence data used in the calculation of effluent dose volume for the septic tanks at sites A and B are archived and are available by request from the USGS New Mexico Water Science Center. The mean daily volume of effluent dosed to the disposal field at site A from April 2011 to December 2012 was 356 L/d; the standard deviation of the daily dose was 121 L/d, and the median daily dose was 344 L/d. At site B, the mean daily volume of effluent dosed to the disposal field from April 2011 to March 2012 was 382 L/d; the standard deviation of the daily dose was 204 L/d, and the median daily dose was 409 L/d. On average, there were four cycles per day with each pump cycle lasting approximately 25 sec (fig. 8). Although the mean daily volume of effluent dosed to the disposal field at site A was similar to site B, the residents at site B frequently took short vacations, with periods of low water use resulting in a higher standard deviation from the mean for site B compared to site A.

Field-Measured Evapotranspiration

During 2011–12, ET chamber measurements were made over 14 separate days at fixed locations on the disposal fields (site A locations 3–7; site B locations 1–7; fig. 5) and on the surrounding terrain (site A locations 1–2 and 8–9; site B locations 8–11; fig. 5). Measurements were made at various times during the growing season (each year between May 19 and November 30) and throughout the day (from 0615 hours to 2000 hours) to capture the seasonal and daily variability in ET rates at the selected locations (table 3); for example, figure 12 shows ET chamber measurements collected at fixed locations along the established cross section at site A on May 19, 2012, from 1820 hours to 2000 hours and on July 14, 2012, from 1750 hours to 1940 hours. On both of these days, three 30-min cross sections were conducted. Discrete measurements of actual ET during July were 2 to 3 times greater than discrete measurements of actual ET during May. In general, actual ET on the disposal field was greater than actual ET on the surrounding terrain, and actual ET above the effluent-distribution lines (laterals 1–3) was greater than actual ET between the effluent-distribution lines. Although each effluent-distribution line received effluent once a day, the timing of effluent doses was not apparent in the volumetric soil-water content data; therefore, it is likely that spatial variability in the actual ET observed on the disposal field is mainly due to the proximity of the measurement location to an effluent-distribution line and variability in vegetation type density.

In total, 360 discrete ET chamber measurements were conducted on 14 different dates from fixed locations at sites A and B; 220 ET chamber measurements were conducted

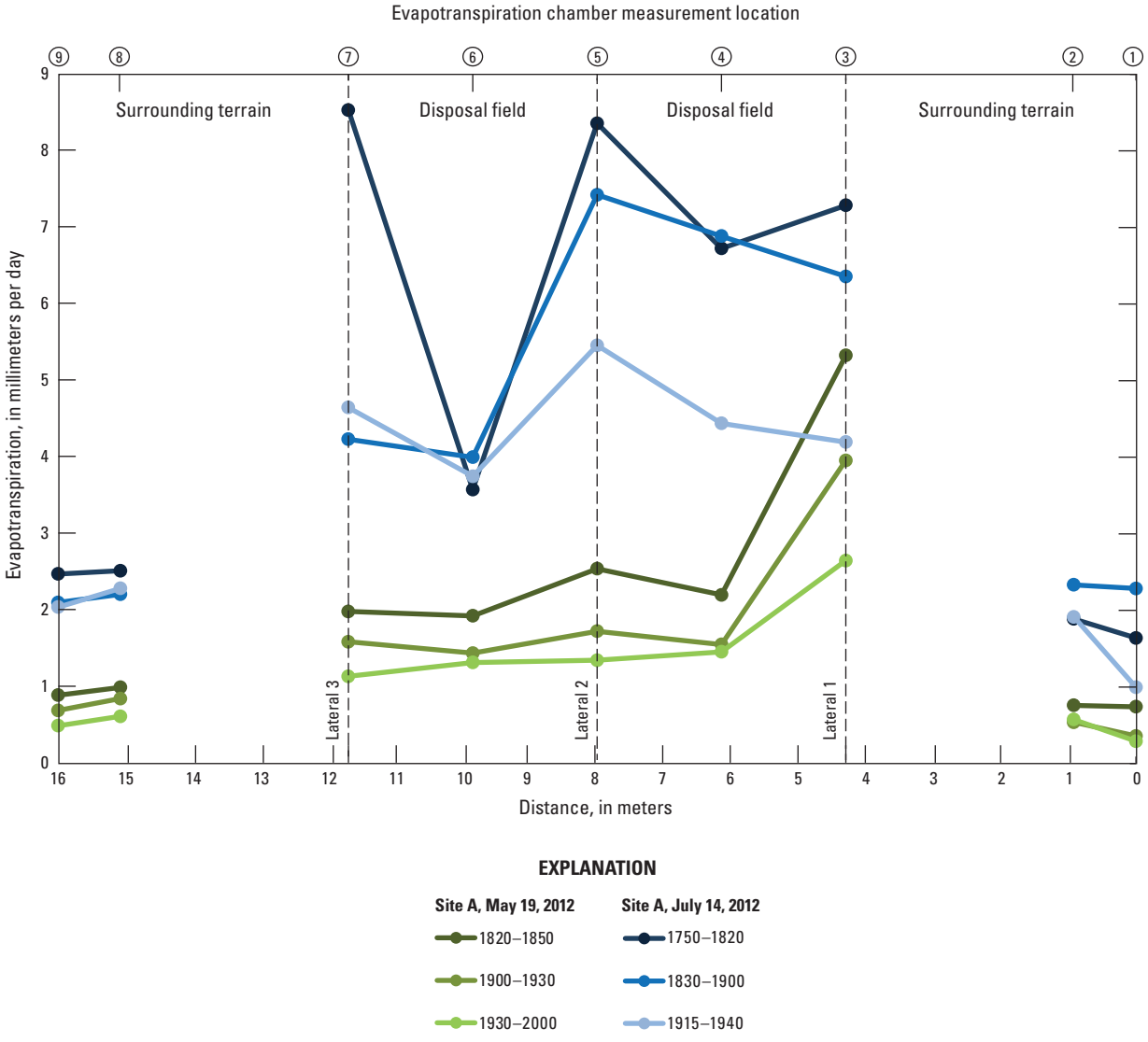

Figure 12. Actual evapotranspiration measured at evapotranspiration chamber measurement locations on the disposal field and the surrounding terrain for site A from approximately 1750 hours to 2000 hours on May 19, 2012, and July 14, 2012.

on the disposal field, and 140 ET chamber measurements were conducted on the surrounding terrain (table 3). The ET chamber measurement data were used to compute actual ET for each measurement location. A summary of all ET chamber measurement data, including time, location, the maximum slope of the vapor density time series, and the computed value of actual ET, can be found in appendix 3. Actual ET data were averaged to compute a mean actual ET in the following manner. During each 30-min cross section at site A, a mean actual ET was computed for the first 2 measurement locations (1–2) and the last 2 measurement locations (8–9) on the surrounding terrain; because these mean measurements occurred approximately 15–20 min apart, each mean was matched to corresponding 15-min time interval micrometeorological and soil data and used to calibrate the influence functions. For locations on the disposal field, a single mean actual ET was computed for all five measurement locations (3–7). Because this mean measurement spanned a 30-min time interval, this mean was matched to the corresponding 15-min time interval micrometeorological and soil data and used to calibrate the influence functions; for example, the mean actual ET computed for site A on May 19, 2012, during the 30-min data-collection period from 1820 hours to 1850 hours (based on data shown in fig. 12) was 0.74 and 0.93 mm/d for the surrounding terrain and 2.79 mm/d for the disposal field. A similar methodology was applied to compute mean actual ET for each 30-min cross section at site B, and these mean values were used to calibrate the influence functions.

Figure 13 shows the mean actual ET computed for the disposal field and the surrounding terrain at sites A and B and total daily precipitation during 2011−12. The mean actual ET on the disposal field ranged from 10.51 mm/d (site A, September 14, 2011) to 0.74 mm/d (site A, November 30, 2011), and the mean actual ET on the surrounding terrain ranged from 4.93 mm/d (site A, September 14, 2011) to 0.25 mm/d (site A, June 14, 2012) (fig. 13).

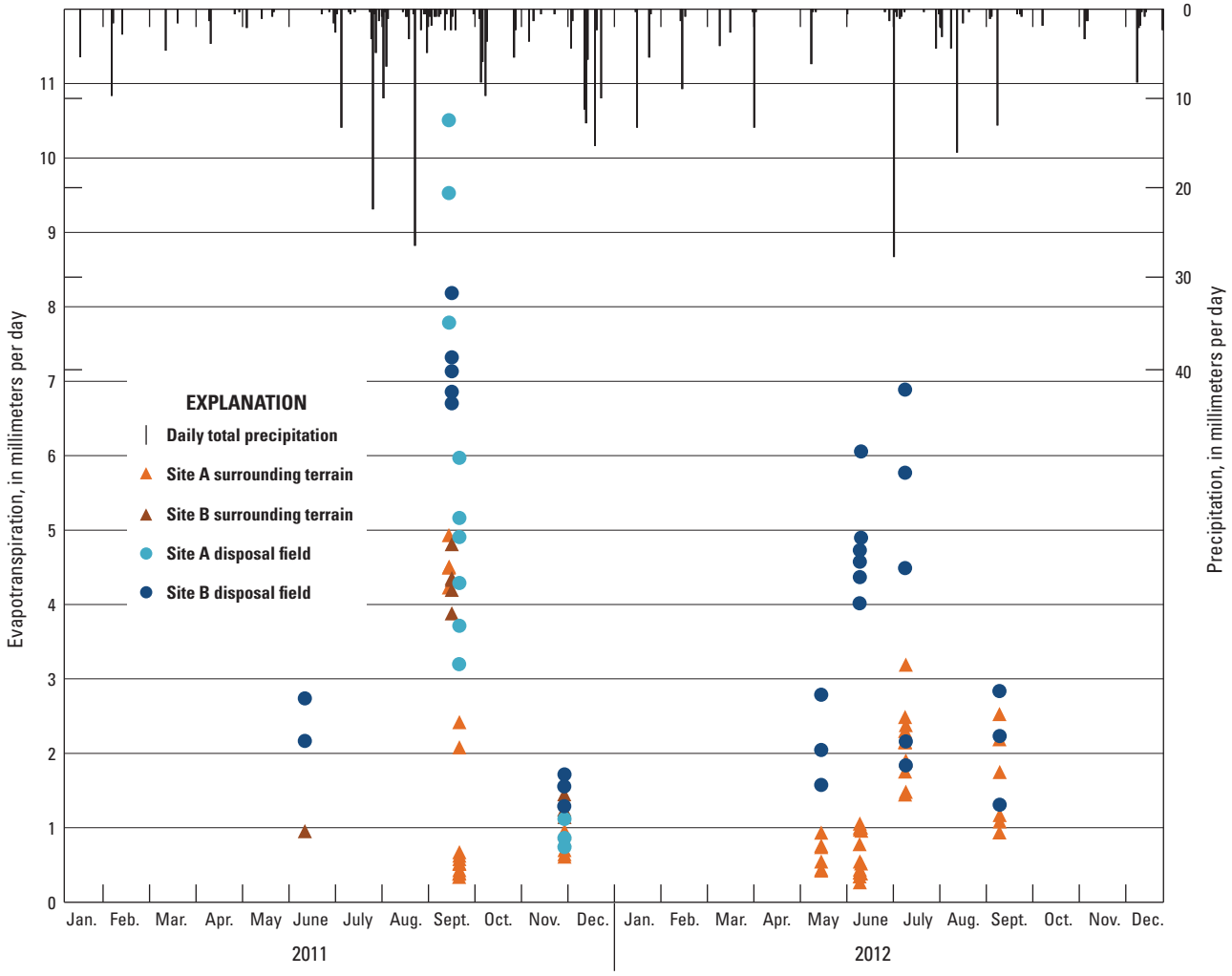

Figure 13. The mean actual evapotranspiration computed for the disposal field and for the surrounding terrain at sites A and B and the daily total precipitation at site A, 2011–12.

Model-Estimated Evapotranspiration

The PM equation was used to model ET on the disposal field and on the surrounding terrain at site A from January 1, 2011, to December 31, 2012, and at site B from January 1, 2011, to December 31, 2011. Mean daily ET was computed each year for the typical growing season (March 15 to November 15) and either computed or estimated each year for the nongrowing season (November 16 to March 14). Evapotranspiration computed during the typical growing season was determined on a 15-min time step and with the mean ET computed daily. The mean daily ET during the nongrowing season was computed by using the model, except where model-computed values were below 0.2 mm/d; the daily ET was then estimated as 0.2 mm/d for both the disposal field and the surrounding terrain by following Stannard and others (2010).

Evapotranspiration was modeled for the disposal fields and the surrounding terrain by using continuous 15-min mean micrometeorological and soil measurements. Modeled ET values were calibrated by using mean actual ET computed from ET chamber measurements at fixed locations on the disposal field and on the surrounding terrain at sites A and B during 2011–12. Data from ET chamber measurements at sites A and B were combined to calibrate influence functions used to estimate the values of canopy conductance (g_c) and soil surface conductance (g_e) in the PM equations for the disposal fields and the surrounding terrain. Parameters used in the model computations are presented in table 4.

The mean daily effluent loss through ET from disposal fields was estimated as the mean daily ET on the disposal field in excess of the mean daily ET on the surrounding terrain. At site A during 2011, the mean daily ET on the disposal field was 1.62 mm/d, and the mean daily ET on the surrounding terrain was 0.43 mm/d (table 5), with a resulting mean daily ET from effluent of 1.19 mm/d (fig. 14*A*). At site A during 2012, the mean daily ET on the disposal field was 1.35 mm/d, and the mean daily ET on the surrounding terrain was 0.45 mm/d (table 5), with a resulting mean ET from effluent of 0.90 mm/d (fig. 14*A*). At site B during 2011, the mean daily ET on the disposal field was 1.42 mm/d, and the mean ET on the surrounding terrain was 0.41 mm/d (table 5), with a resulting mean ET from effluent of 1.01 mm/d (fig. 14*B*; table 5).

Assessment of Model-Estimated Evapotranspiration

Values of mean actual ET were compared to mean modeled ET for the same time period to assess the accuracy of ET values predicted by the model (fig. 15*A* and 15*B*). The goodness of fit between modeled and measured values was assessed by using the CE (table 4), in which values closer to one indicate a higher correlation and goodness of fit between modeled and measured values of ET. The goodness of fit between modeled and measured ET was better for the disposal field (CE=0.79, R^2=0.79) than for the surrounding terrain (CE=0.37, R^2=0.45). Because the PM model is based on a "big leaf" assumption, the poor fit between modeled and measured ET for the surrounding terrain shown in figure 15*B* was likely due to the sparseness of vegetation.

The seasonal and annual variability in micrometeorological and soil conditions, particularly soil-water content, are factors that should be assessed when determining how well model estimations of ET compare to actual ET. Other factors, such as spatial variability in soil properties, differences in disposal field design, and variations in vegetation type and density, can also increase uncertainty in model results. Rana and Katerji (1998) state that for a well-irrigated field (disposal field in this study), the accuracy of the available energy and aerodynamic resistance measurements are of greatest importance to modeled ET; however, under water-stressed conditions (surrounding terrain in a semiarid climate), the canopy and soil surface aerodynamic resistance becomes the most important term to evaluate. In general, the PM model was most sensitive to net radiation, vapor pressure deficit, and wind speed.

Table 5. Summary of the values used to compute the mean daily volume of effluent available for potential recharge from the disposal fields at sites A and B, 2011–12.

[ET, evapotranspiration; DF, disposal field; mm/d, millimeters per day; ST, surrounding terrain; m^2, square meter; L/d; liter per day]

Station	Period of data collection	Mean daily ET on the DF (mm/d)	Mean daily ET on the ST (mm/d)	Mean daily ET due to effluent (mm/d)	Effective effluent-drainage area of DF (m^2)	Mean daily volume of effluent dosed to DF (L/d)	Mean daily volume of effluent lost to ET from DF (L/d)	Mean daily volume of effluent available for potential recharge from DF (L/d)	Percent of dose available for potential recharge
Site A	2011	1.62	0.43	1.19	150.6	356	174	182	51
Site A	2012	1.35	0.45	0.90	150.6	356	132	224	63
Site B	2011	1.42	0.41	1.01	117.1	382	99	283	74

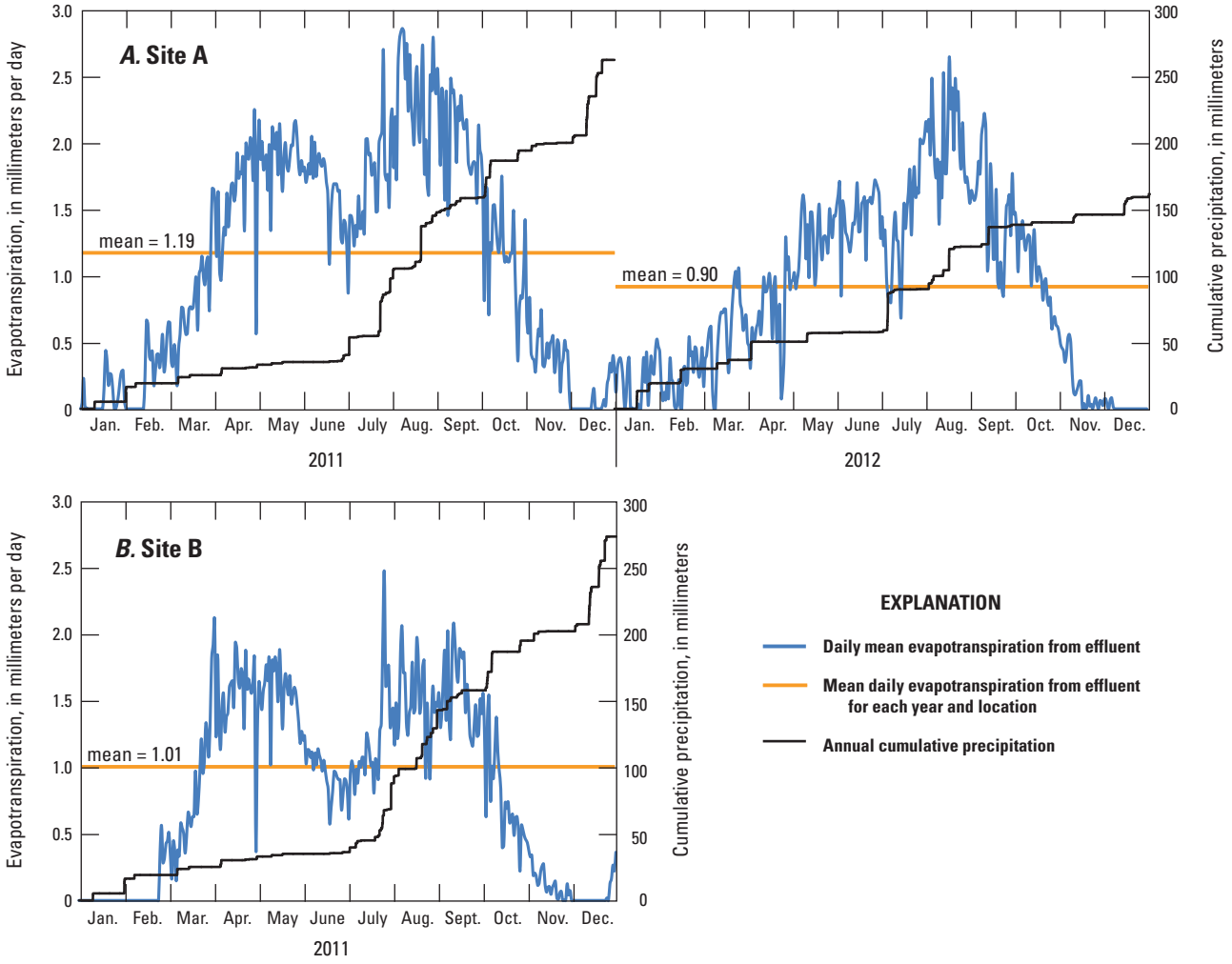

Figure 14. The daily mean evapotranspiration from effluent, mean daily evapotranspiration values based on year and location, and cumulative yearly precipitation at *A*, site A, 2011–12; and *B*, site B, 2011.

Factors affecting actual ET at discrete measurement locations include precipitation, the distance between adjacent effluent-distribution lines, the depth of the lateral trenches, and the proximity of the soil-water-content probes to an effluent-distribution line. The volumetric soil-water content on the disposal field at site A was less responsive to precipitation events in 2012 compared to 2011, possibly because of less precipitation (40 percent less) in 2012 than in 2011 (fig. 16). The volumetric soil-water content of soil core samples collected on the disposal fields at sites A and B in August 2010 provided additional information about the soil drainage following a precipitation event. The volumetric soil-water content measured in the lower portion of the cores indicated that drainage occurred below the disposal field, but it is not clear if the moisture was due to downward percolation of precipitation beyond the root zone, the drainage of effluent, or a combination of both, or if lateral movement of water along the surface of the underlying fractured limestone bedrock was a factor. After large precipitation events (greater than 10 mm), the volumetric soil-water content at sites A and B return to field capacity relatively quickly (after a few days).

As noted in the methods section, the TDR sensors installed on the disposal field and on the surrounding terrain at sites A and B represented an "average" location, with the disposal field TDR sensor located approximately halfway between the lateral lines. On average, four doses were delivered to the disposal field each day, such that each lateral (3 laterals at site A and 4 laterals at site B) received a dose of effluent about once daily. The timing between doses of effluent to each lateral is sufficiently short (once daily), and large diurnal fluctuations in volumetric soil-water content are not seen in sensor data from the disposal field, indicating that the TDR sensor would not be expected to experience large volumetric soil-water content changes that are not representative of the mean field conditions. This could be a major factor contributing to the rather poor model fit to measure ET.

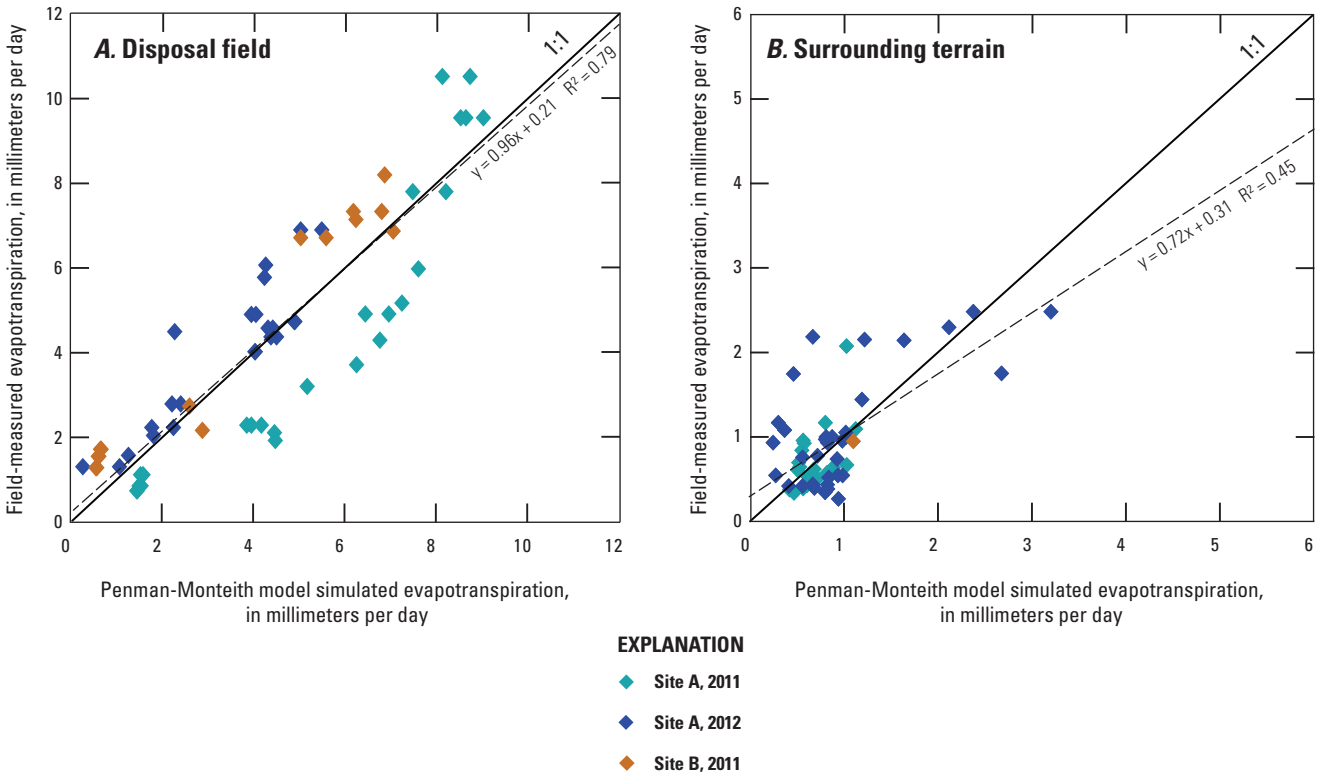

Figure 15. Comparison of Penman-Monteith model simulated evapotranspiration and field-measured evaportanspiration on *A*, the disposal field, and *B*, the surrounding terrain at sites A and B, 2011–12.

Variability in vegetation density at site A between 2011 and 2012 was also a factor affecting relations between measured and modeled ET. The removal of vegetation from the disposal field at site A during June 2011 to reduce the risk of wildfire might have affected model estimations of ET on the disposal field for that year. A single LAI curve was used for both years, which does not account for human changes to vegetation density on the disposal field. This change in vegetation density and our single LAI curve may have led to the model overestimation of ET that can been seen in figure 15*A*, in which the majority of points in 2011 at site A plot below the 1:1 line, compared to points in 2012 at site A when the disposal field was left untouched throughout the year. Variability between the modeled and measured ET values was large in 2011 for the disposal field at site A. In figure 15*A*, the underestimation of modeled ET with respect to measured values (points plotting above the 1:1 line) at site A during 2011 was likely due to a series of small precipitation events over a period of days before the ET measurements were taken. It is likely that these precipitation events increased the moisture of the soil near land surface (what the ET chamber measured); however, this moisture may not have percolated to a depth of 2.5–5.5 cm below land surface (what the TDR sensor measured), causing the ET model to underestimate the value of ET as compared to measured ET values.

Estimation of Groundwater Recharge from Effluent

The mean daily volume of potential recharge due to effluent was estimated as the mean daily volume of effluent dosed to the disposal field in excess of the mean daily volume of effluent loss from ET from the disposal field (based on daily mean ET values in appendix 4). The mean daily ET loss from effluent was multiplied by the effective drainage area of the disposal field to obtain the mean daily volume of effluent loss from ET from the disposal field. The effective drainage area was estimated by using field-measured ET and observations of vegetation density; however, computations of recharge are directly proportional to estimates of recharge area and are a large source of uncertainty. For site A during 2011, the mean daily volume of effluent loss from ET from the disposal field was 174 L/d, and the resulting effluent available for potential recharge was 182 L/d (or 51 percent of the volume of effluent dosed to the disposal field) (table 5). For site A during 2012, the mean daily volume of effluent loss from ET from the disposal field was 132 L/d, and the resulting effluent available for potential recharge was 224 L/d (or 63 percent of the volume of effluent dosed to the disposal field). Lastly, for site B in 2011, the mean daily volume of effluent loss from ET

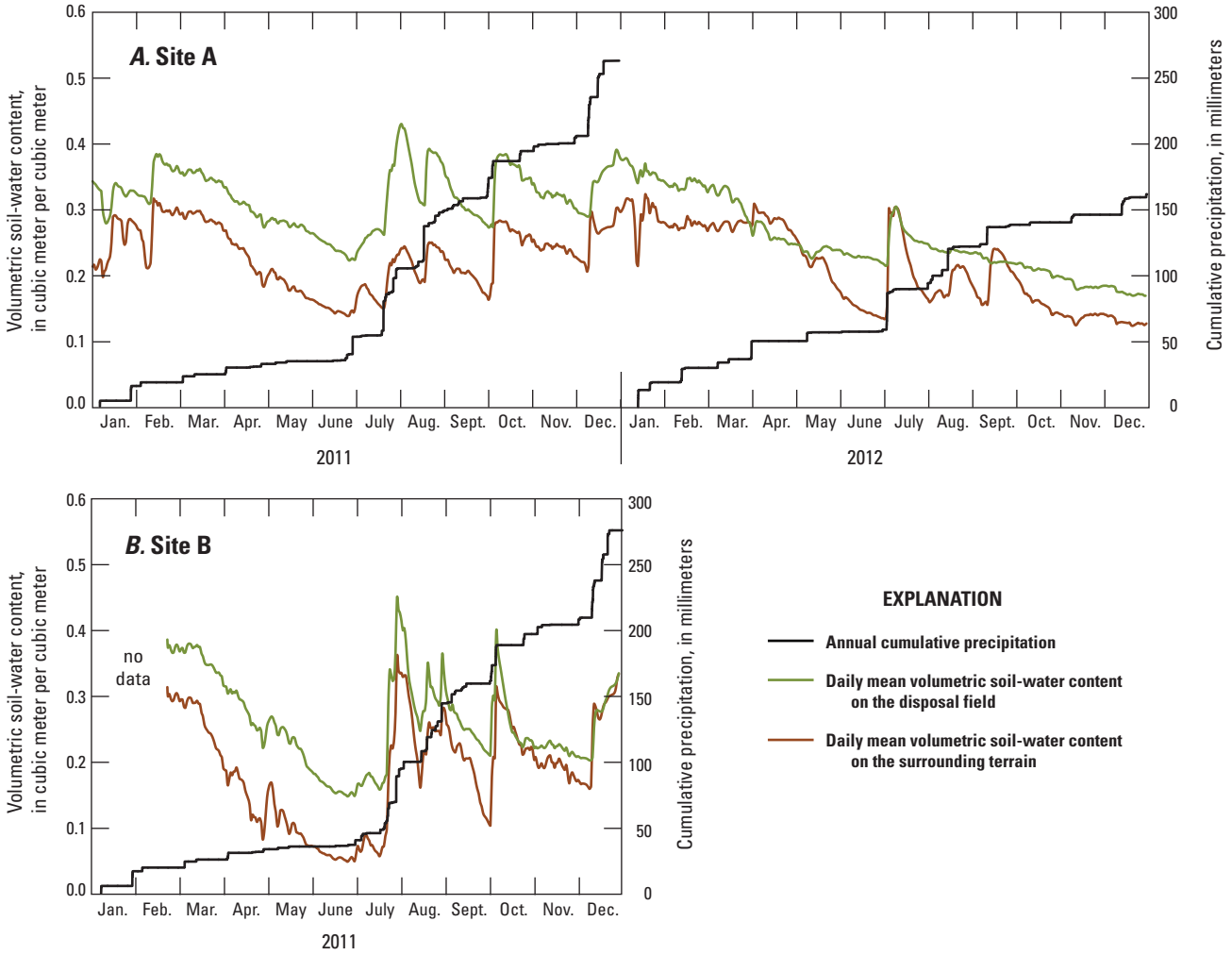

Figure 16. *A*, the daily mean volumetric soil-water content and annual cumulative precipitation at study site A, 2011–12, and *B*, the daily mean volumetric soil-water content and annual cumulative precipitation at study site B, 2011.

from the disposal field was 99 L/d, and the resulting effluent available for potential recharge was 283 L/d (or 74 percent of the volume of effluent dosed to the disposal field). This study found that the mean percentage of a dose available for potential recharge is 63 percent.

As of 2010, there were approximately 19,000 people and approximately 9,000 households (U.S. Census Bureau, 2010) in the EMA of eastern Bernalillo County, which results in an average population per household of 2.1 people. The mean volume of effluent dosed to the disposal field for a two-person household in this study was 369 L/d. By using these estimates, the total effluent dosed to disposal fields per day in eastern Bernalillo County is about 3.5 million L/d, or about 1,027 acre-feet per year. If 63 percent of the mean amount of effluent dosed to a disposal field contributes to drainage in eastern Bernalillo County, then the maximum potential recharge is about 2.2 million L/d, or about 647 acre-feet per year.

Summary

Eastern Bernalillo County, New Mexico, is a historically rural area that in recent years has experienced an increase in population and in the construction of new housing units, most of which are not connected to a centralized wastewater treatment system. Increasing water use has raised concerns about the effect of development on the available groundwater resources in the area. During 2011–12, the U.S. Geological Survey, in cooperation with Bernalillo County Public Works Natural Resource Services, used a water-budget approach to quantify the potential groundwater recharge occurring from the domestic sewage (effluent) dosed to the sewage disposal field (disposal field) at two locations—sites A and B—located in eastern Bernalillo County, N. Mex. During this study, the disposal fields at sites A and B received effluent from two-person domestic residences equipped with an onsite low-pressure dosing system. The mean daily volume of effluent

dosed to the disposal field at sites A and B that is potentially available for recharge was determined as the mean daily volume of effluent dosed to the disposal field in excess of the mean daily volume of effluent loss from evapotranspiration (ET) from the disposal field. The amount of effluent loss from ET from the disposal field was estimated as the amount of ET loss from the disposal field in excess of ET loss on the surrounding terrain. The mean daily volume of effluent dosed to the disposal field was estimated by using the product of the horizontal surface area of the septic tank and the total daily effluent-level decrease within the septic tank. A combined ET measurement and modeling technique was used to estimate the amount of ET loss from the disposal field and from the surrounding terrain. Micrometeorological and soil data from instrumentation on the disposal fields and on the surrounding terrain at sites A and B were used as input data into the Penman-Monteith equation. Annually, ET loss on the disposal fields and on the surrounding terrain at sites A and B was computed on a 15-minute time step. A portable hemispherical flux chamber (ET chamber) was used to measure ET at fixed locations on the disposal fields and on the surrounding terrain at sites A and B. During 2011–12, 360 discrete ET chamber measurements were conducted on 14 different dates from fixed measurement locations on the disposal fields and on the surrounding terrain at sites A and B. These measurements were conducted at various times during the year and at various times during the day to capture the seasonal and daily variability in ET rates at the fixed locations. Data from ET chamber measurements were used to calibrate a Penman-Monteith modeled ET rate on the surrounding terrain at site A from January 1, 2011, to December 31, 2011, and from January 1, 2012, to December 31, 2012, and at site B from January 1, 2011, to December 31, 2011.

The mean daily volume of effluent dosed was 356 liters per day at site A from April 2011 to December 2012 and was 382 liters per day at site B from April 2011 to March 2012. Mean actual ET was computed from ET chamber measurements collected at fixed locations on the disposal field and on the surrounding terrain at sites A and B during 2011–12. Of the ET chamber measurements collected during 2011−12 at sites A and B, the mean actual ET on the disposal field ranged from 10.51 millimeters per day (mm/d) on September 14, 2011, to 0.74 mm/d on November 30, 2011, and the mean actual ET on the surrounding terrain ranged from 4.93 mm/d on September 14, 2011, to 0.25 mm/d on June 14, 2012. The Penman-Monteith equation was used to model ET on the disposal field and on the surrounding terrain at site A from January 1, 2011, to December 31, 2012, and at site B from January 1, 2011, to December 31, 2011. Mean actual ET was used to calibrate model ET values. The mean daily ET on the disposal fields was 1.62 mm/d and 1.42 mm/d during 2011 at sites A and B, respectively, and was 1.35 mm/d during 2012 at site A. The mean daily ET on the surrounding terrain was 0.43 mm/d and 0.41 mm/d during 2011 at sites A and B, respectively, and was 0.45 mm/d during 2012 at site A. The estimated amount of effluent loss from ET on the disposal field was 1.19 mm/d and 1.01 mm/d during 2011 at sites A and B, respectively, and was 0.90 mm/d during 2012 at site A. The mean potential recharge from disposal field effluent during 2011–12 was 63 percent of the volume of effluent dosed to the disposal field (average of 51, 63, and 74 percent).

References Cited

Allen, R.G., Walter, I.A., Elliott, R.L., Howell, T.A., Itenfisu, Daniel, Jensen, M.E., and Snyder, R.L., 2005, The ASCE standard reference evapotranspiration equation: American Society of Civil Engineers, Reston, Va., 216 p.

Bartolino, J.R., Anderholm, S.K., and Myers, N.C., 2010, Groundwater resources of the East Mountain area, Bernalillo, Sandoval, Santa Fe, and Torrance Counties, New Mexico, 2005: U.S. Geological Survey Scientific Investigations Report 2009–5204, 88 p. [Also available at http://pubs.usgs.gov/sir/2009/5204/.]

Berger, D.L., Johnson, M.J., Tumbusch, M.L., and Mackay, Jeffrey, 2001, Estimates of evapotranspiration from the Ruby Lake National Wildlife Refuge Area, Ruby Valley, northeastern Nevada, May 1999–October 2000: U.S. Geological Survey Water-Resources Investigations Report 01–4234, 38 p. [Also available at http://pubs.usgs.gov/wri/wri014234/.]

Bernalillo County Public Works Natural Resource Services, 2013, Septic tank geospatial data: Bernalillo County, Albuquerque, N. Mex., [computer file].

Bittelli, M., Salvatorelli, F., and Pisa, P.R., 2008, Correction of TDR-based soil water content measurements in conductive soils: Geoderma, v. 143, p. 133–142.

Blanchard, P.J., and Kues, G.E., 1999, Ground-water quality and susceptibility of groundwater to effects from domestic wastewater disposal in eastern Bernalillo County, central New Mexico, 1990–91: U.S. Geological Survey Water-Resources Investigations Report 99–4096, 109 p. [Also available at http://pubs.usgs.gov/wri/1999/4096/report.pdf.]

Blandford, T.N., 2006, Evaluation of return flow from municipal type domestic water uses for return flow credits application RA–130 et al.: Daniel B. Stephens and Associates consulting report prepared for Berrendo Cooperative Water Users Association, Roswell, N. Mex., 20 p.

Campbell Scientific, Inc., 1987, Bowen ratio instrumentation, instruction manual—Revision 9/05: Campbell Scientific, Inc., Logan, Utah, 36 p. [Also available at http://s.campbellsci.com/documents/us/manuals/bowen.pdf.]

Campbell Scientific, Inc., 1998, NR-Lite2 net radiometer, instruction manual—Revision 3/13: Campbell Scientific, Inc., Logan, Utah, 30 p. [Also available at http://s.campbellsci.com/documents/us/manuals/nr-lite2.pdf.]

Campbell Scientific, Inc., 2002a, CS616 and CS625 water content reflectometers, instruction manual—Revision 3/12: Campbell Scientific, Inc., Logan, Utah, 44 p. [Also available at http://s.campbellsci.com/documents/us/manuals/cs616.pdf.]

Campbell Scientific, Inc., 2002b, Model HFP01 soil heat flux plate, instruction manual—Revision 7/12: Campbell Scientific, Inc., Logan, Utah, 44 p. [Also available at http://s.campbellsci.com/documents/us/manuals/hfp01.pdf.]

Das, B.M., 2009, Soil mechanics laboratory manual (7th ed.): Oxford University Press, 299 p.

Hansen, F.V., 1993, Surface roughness lengths: U.S. Army Research Laboratory, ARL–TR–61, 22 p.

Healy, R.W., 2010, Estimating groundwater recharge: Cambridge, Cambridge University Press, 264 p.

Helsel, D.R., and Hirsch, R.M., 2002, Statistical methods in water resources: U.S. Geological Survey Techniques of Water-Resources Investigations, book 4, chapter A3, 522 pages.

Lowe, P.R., 1977, An approximating polynomial for the computation of saturation vapor pressure: Journal of Applied Meteorology, v. 16, no. 1, p. 100–103.

McQuillan, D.M., and Bassett, E.C., 2009, Return flow to groundwater from onsite wastewater systems—Proceedings of the National Onsite Wastewater Recycling Association 18th Annual Technical Conference and Expo: April 6–9, 2009, Milwaukee, Wis., National Onsite Wastewater Recycling Association, 9 p. [Also available at http://www.nmenv.state.nm.us/fod/LiquidWaste/documents/McQuillanandBassettNOWRA09.pdf.]

Monteith, J.L., and Unsworth, M.H., 1990, Principles of environmental physics (2nd ed.): Edward Arnold, London, 291 p.

Nash, J.E., and Sutcliffe, J.V., 1970, River flow forecasting through conceptual models part 1—A discussion of principles: Journal of Hydrology, v. 10, no. 3, p. 282–290.

New Mexico Office of the State Engineer, 2001, Order in the matter of the application by Fambrough Water Cooperative Association for permit request for return flow credit for diversion of ground water within the Roswell artesian underground water basin in New Mexico: Hearing no. 99-660, OSE File no. RA-406-A-A, 8 p. [Also available at http://www.ose.state.nm.us/water-info/hearing-decisions/hu99-060.pdf.]

Rainwater, K., Jackson, A., Ingram, W., Lee, C., Thompson, D., Mollhagen, T., Ramsey, H., and Urban, L., 2005, Field demonstration of the combined effects of absorption and evapotranspiration on septic system drainfield capacity: Water Environment Research, v. 77, no. 2. p. 150–169.

Rana, G., and Katerji, N., 1998, A measurement-based sensitivity analysis of Penman-Monteith actual evapotranspiration model for crops of different height and in contrasting water status: Theoretical Applied Climatology, v. 60, p. 141–149.

Sherlock, M.D., McDonnell, J.J., Curry, D.S., and Zumbuhl, A.T., 2002, Physical controls on septic leachate movement in the vadose zone at the hillslope scale, Putnam County, New York, USA: Journal of Hydrological Processes, v. 16, no. 13, p. 2559–2575.

Shuttleworth, J.W., 2008, Evapotranspiration measurement methods: Southwest Hydrology, v. 7, no. 1, p. 23. [Also available at http://web.sahra.arizona.edu/swhydro/archive/V7_N1/feature3.pdf.]

Stannard, D.I., 1988, Use of a hemispherical chamber for measurement of evapotranspiration: U.S. Geological Survey Open-File Report 88–452, 18 p. [Also available at http://pubs.usgs.gov/of/1988/0452/report.pdf.]

Stannard, D.I., 1993, Comparison of Penman-Monteith, Shuttleworth-Wallace, and modified Priestley-Taylor evapotranspiration models for wildland vegetation in semiarid rangeland: Water Resources Research, v. 29, no. 5, p. 1379–1392.

Stannard, D.I., 1997, A theoretically based determination of Bowen-ratio fetch requirements: Boundary-Layer Meteorology, v. 83, p. 375–406.

Stannard, D.I., Paul, W.T., Laws, R., Poeter, E.P., 2010, Consumptive use and resulting leach-field water budget of a mountain residence: Journal of Hydrology, v. 388, p. 335–349.

Tuan, Yi-Fu, Everard, C.E., and Widdison, J.G., 1969, The climate of New Mexico: New Mexico State Planning Office, 169 p.

U.S. Census Bureau, 1990, Census 1990 summary file, census tracts 38.03–38.07, New Mexico: U.S. Census Bureau, accessed November 4, 2011, at http://www.census.gov/dmd/www/90census.html.

U.S. Census Bureau, 2010, Census interactive population search, census tracts 38.03–38.07, New Mexico: U.S. Census Bureau, accessed August 23, 2013, at http://www.census.gov/2010census/popmap/ipmtext.php?fl=35.

U.S. Department of Agriculture, 1987, Soil mechanics level 1, module 3—USDA Textural Soil Classification: U.S. Department of Agriculture, Soil Conservation Service, accessed August 8, 2013, at ftp://ftp.wcc.nrcs.usda.gov/wntsc/H&H/training/soilsOther/soil-USDA-textural-class.pdf.

U.S. Department of Agriculture, 2012, Web soil survey for New Mexico, Bernalillo County and parts of Sandoval and Valencia Counties: U.S. Department of Agriculture, Natural Resources Conservation Service, accessed April 22, 2012, at http://websoilsurvey.nrcs.usda.gov/app/.

U.S. Environmental Protection Agency, 1999, Decentralized system technology fact sheet—Low pressure pipe systems: EPA 832-F-99-076, 7 p., accessed January 6, 2011, at http://water.epa.gov/scitech/wastetech/upload/2002_09_23_mtb_finallpp.pdf.

Weather Underground, 2012, Daily weather history, station KNMEDGEW7 (Edgewood, New Mexico) from 2010 to 2012: Weather Underground, accessed May 7, 2013, at http://www.wunderground.com/personal-weather-station/dashboard?ID=KNMEDGEW7.

Weather Underground, 2013, Daily weather history, station KNMTIJER2 (Tijeras, New Mexico) from 2010 to 2012: Weather Underground, accessed May 7, 2013, and August 8, 2013, at http://www.wunderground.com/weatherstation/WXDailyHistory.asp?ID=KNMTIJER2.

Western Regional Climate Center, 2013a, Average annual class A pan evaporation data for station 293060 (Estancia, New Mexico) from 1914 to 2005: Western Regional Climate Center, accessed August 8, 2013, at http://www.wrcc.dri.edu/htmlfiles/westevap.final.html#NEW MEXICO.

Western Regional Climate Center, 2013b, Monthly climate summary, station 293060 (Estancia, New Mexico) from 1914 to 2005: Western Regional Climate Center, accessed August 8, 2013, at http://www.wrcc.dri.edu/cgi-bin/cliMAIN.pl?nmesta.

Wilson, B.C., and Lucero, A.A., 1997, Water use by categories in New Mexico counties and river basins, and irrigated acreage in 1995: New Mexico Office of the State Engineer, Technical Report 49, 149 p., accessed April 12, 2012, at http://www.ose.state.nm.us/PDF/Publications/Library/TechnicalReports/TechReport-049.PDF.

Wilson, B.C., Lucero, A.A., Romero, J.T., and Romero, P.J., 2003, Water use by categories in New Mexico counties and river basins, and irrigated acreage in 2000: New Mexico Office of the State Engineer, Technical Report 51, 164 p., accessed April 12, 2012, at http://www.ose.state.nm.us/PDF/Publications/Library/TechnicalReports/TechReport-051.pdf.

Publishing support provided by
Lafayette Publishing Service Center

ISSN 2328-0328 (online)
http://dx.doi.org/10.3133/sir20155060